

1 Answer to review 1

Interactive comment on “Classification of Arctic multilayer clouds using radiosoundings and radar data” by Maiken Vassel et al.

Anonymous Referee #1

Received and published: 28 September 2018

Review of “Classification of Arctic multilayer clouds using radiosoundings and radar data” by Vessel et al.

We thank the anonymous reviewer for his/her review and the detailed comments. We have revised the manuscript accordingly, including a revision of all sublimation calculations, updates of all figures, and major changes of the text. Our replies to your comments are given below in blue after the specific comment. Our page references refer to the corrected version of the paper.

Recommendation: Might be acceptable for publication after mandatory revision

This paper analyzes a year of data collected by a radar and radiosoundings at Ny-Alesund and attempts to determine the frequency of occurrence of multi-layer clouds, and in the case of multi-layer clouds whether the cloud layer underneath is seeded by the cloud above. The subject matter is timely because the Arctic is currently warming quicker than other parts of the planet, yet models have a difficult time accurately predicting the amount of warming. Better knowledge of the properties of arctic clouds, and on what controls them, is necessary in order to improve these predictions: any paper that hence contributes to our data base on the phases, heights and geometrical characteristics of clouds is beneficial. The paper is well written and the presented analysis easy to understand. Nevertheless, I fear that the paper as currently written is quite misleading. There are so many uncertainties and problems with the analysis (which, in their defense, the authors do a good job of identifying) that I fear the results that come out of the paper are not terribly useful. However, I think if the data were presented in an alternate way the study could be of potential use and hence I am recommending major revision rather than rejection.

Step 1 of their analysis uses the radiosonde data to identify the presence of multi-layer clouds. However, even though the probability of detection of the multi-layer clouds is 99% with this method, the false alarm rate of 58% “reveals that about half of the MLC detected by radiosounding is no MLC by radar.” Thus, it seems that the paper should be reworded to emphasize that the use of the radiosonde data on its own does not reliably identify the occurrence of MLCs, but can be used in combination with radar data to give information on the presence of MLCs. The authors acknowledge the unreliability of the radiosonde data on their own to identify MLCs as they state “even if the layers above and below are supersaturated with respect to ice, the lack of suitable IN can prevent ice cloud formation.” They also stated that “the results obtained by the radiosonde profiles disagree with actual MLC occurrence observed by the radar.”

It is true that we find using only radiosonde data not being the best method to detect cloud layers. The use of radar instead would lead to much more reliable statistics about visible multilayer clouds. For this we refer to Nomokonova et al. [2018]. However, our main idea was to investigate the possibility of seeding in connection with multilayer clouds. In order to do so, a radiosonde profile is essential to calculate the possibility of seeding (using the temperature and humidity profile of the radiosounding). Using primarily radar and in a second step the radiosonde does not solve the problem, since we show that seeding does hardly ever occur in between two in the radar visible cloud layers (cat. 8 in Fig. 8 in Vassel et al. [2018]). That means seeding itself can very poorly be differentiated from a cloud layer in the radar. Because of that we use primarily radiosonde data and radar data only as a further measure, even if this leads to high uncertainties. We have reworded some of the paragraphs in order to make clear that both radiosonde and radar is needed (p.10 l.16-17, p.15 l.16-17).

The second major problem with the analysis presented is the reliance on the chosen ice crystal size to calculate which of the upper layers of MLCs is seeding a lower layer. As stated by the authors “varying the initial ice crystal size has a large, non-linear impact on the distribution between seeding and non-seeding subsaturated layers.” Further, their calculations substantially underestimate the variance that the size of the seeding ice crystal size might have. In several studies of in-situ measurements of mixed-phase clouds, the ice crystal sizes have been much larger than the 150 micrometer size assumed in the calculations here. Further, the calculations assume a hexagonal plate which is not representative of the shapes of ice crystals in mixed-phase clouds. For example, Korolev et al. (1998) found that over 98% of ice crystals in mixed-phase arctic clouds had irregular shapes. Thus, the uncertainties will be much larger than those stated, and the stated uncertainties are already huge. And, the base size of 100 micrometers is probably much smaller than the size of particles that will be emanating from the upper layer.

This is a valid comment, and we have revised the calculations taking into account larger crystal sizes. The upper cloud of a MLC, from where the falling ice crystals origin, can either be a mixed-phase cloud or a cirrus cloud. In mixed-phase clouds Korolev et al. [1999] measured ice crystals with radii of about $r = 400 \mu\text{m}$. We also refer to Fig. 5e in Mioche et al. [2016], where a radius of $r = 400 - 500 \mu\text{m}$ can occur in mixed-phase clouds. For cirrus clouds Krämer et al. [2009] showed that the radii of ice crystals range between $r = 1 - 100 \mu\text{m}$. In order to account for both cloud types, we have redone our calculations for the ice crystal sizes $r = 100, 200$ and $400 \mu\text{m}$. Our main focus is now on $r = 400 \mu\text{m}$, assuming in most cases the upper cloud to be mixed-phase.

We agree with you that the ice crystal shape should not be treated as a sphere. We changed the calculation and the text accordingly (p.4 and p.6). We have selected the four ice crystal shapes hexagonal plate, rimed particle, stellar and irregular particle which are representative for mixed-phase clouds [Mioche et al., 2016]. For these particles we use the fall speed calculation shown in Fig. 1 and given by Mitchell [1996]. The main focus in the paper is on the hexagonal plate. The results for the other shapes is presented in the Appendix. We do not account for the lower limit of ice crystal size given by Mitchell

[1996], since in our calculation we have to calculate the speed also for very small ice crystals due to sublimation. Note that this might lead to a small error of too fast falling small ice crystals.

We also corrected the capacitance. We are now using the calculation of Westbrook et al. [2008]. The cases selected are listed in A1 of the paper, as well as the aspect ratios chosen by us.

In Fig. 2 we present the variation of the different ice crystal shapes on the result of classification step 2. As mentioned in the paper, on classification step 1 there is a small variation, but on classification step 2 there is almost no impact of the ice crystal shape on the result (p.10, 1.4 and p.12, 1.14-15).

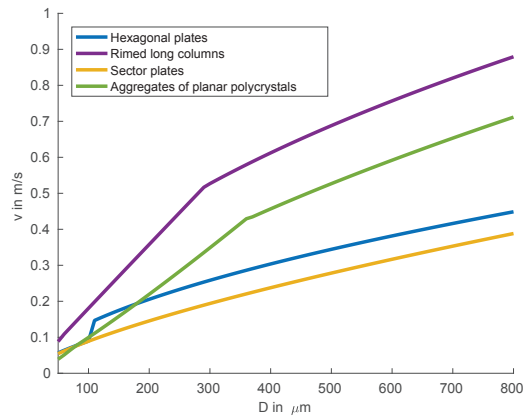


Figure 1: Ice crystal fall speed in dependence of particle size [Mitchell, 1996]

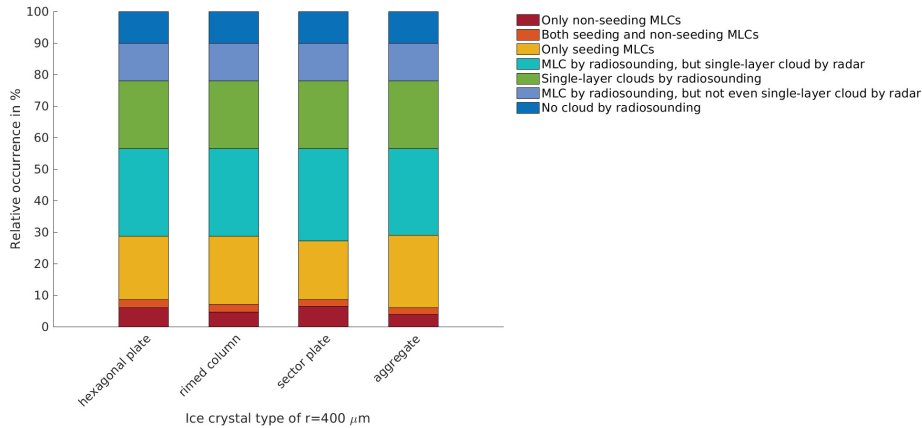


Figure 2: Classification step 2 using different ice crystal shapes with $r = 400 \mu\text{m}$.

Another potential problem could be the lack of colocation between the radiosondes

(which can drift large distances in the background wind) and the radar, which is again noted by the authors: “horizontal drift of the radiosonde away from the radar and inaccuracies due to time averaging of the radar data can explain contradictions between radiosounding and radar.” Was any effort made to consider the advection of air parcels measured by the radiosondes so that the radar data at an appropriate time could be used in the analysis (provided that the air parcel was within the radar view volume at some time)?

In response to this comment, we have revised our calculations. In order to account for the advection, we calculate the wind speed in each layer. Using this information together with the distance between the radiosonde and the radar, we calculate the time the air parcel needs to drift from the radar to the position of the radiosonde. For this we do not consider the wind direction, but assume that the air parcel drifts the same direction as the radiosonde. As an example we show the results of the calculation for 3 November 2016 (Fig. 3). For the 3 November 2016 the average time over all heights is 12.94 min. For our statistics we have added the average time for each day to the time chosen for the evaluation of the radar data. For the 3 November 2016 the resulting radar time period is shown in Fig. 4. The results were changed only marginally by this correction.

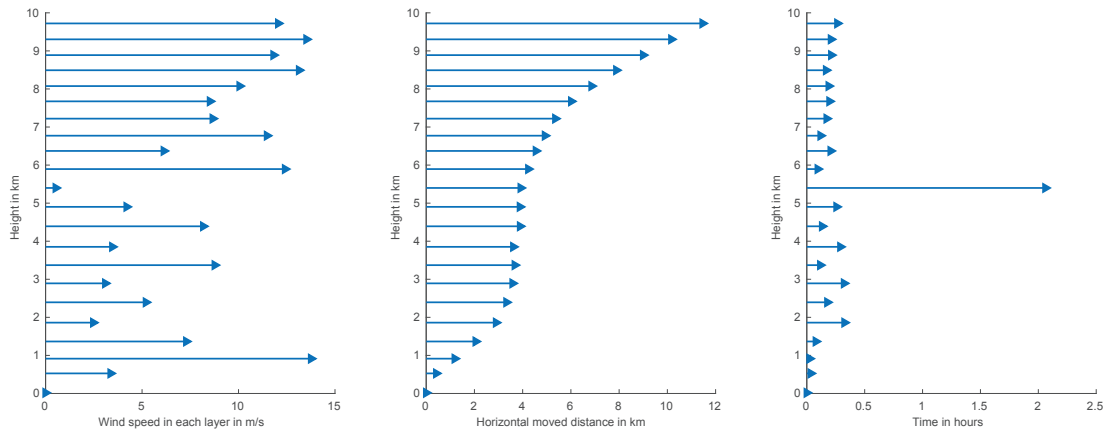


Figure 3: Advection on 3 November 2016: a) windspeed in each height layer, b) estimated distance between radar and radiosonde, c) estimated time that the air parcel needs to drift from the radar to the position of the radiosonde.

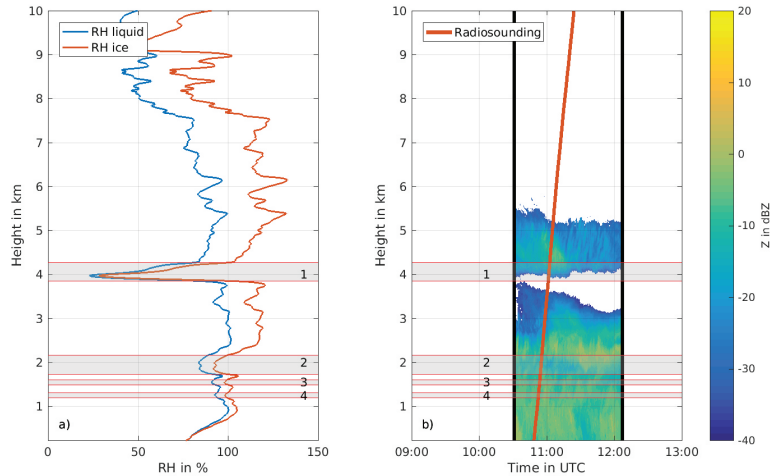


Figure 4: a) Radiosonde data, b) radar time period corrected due to advection

MORE DETAILED COMMENTS:

Abstract: At first reading, I was confused that the 9% and 23% of the cases mentioned because it did not add to 100%. Perhaps mention that other cases (of the 8 categories) are included to avoid confusion.

Thanks for this comment, we added the following bracket to make it clearer: "Seeding cases are found often, in 23 % of the investigated days (100 % includes all days, also non-cloudy days)".

Page 1, Line 24: I find trying to differentiate between the terms multilayered clouds and multilayer clouds (MLC) very confusing! To me, that is the exact same word.

We agree with you that the use of the terms multilayered cloud/multilayer clouds create some confusion at the moment and are not used in a consistent way in literature. Verlinde et al. [2007, 2013] describe a multilayered cloud as a continuous cloud layer with a variable lidar signal inside this cloud layer. It refers to one cloud with different layers. We use the word multilayer clouds referring to separate clouds with clear visible interstice in between. In our case we refer to cloud layers in the atmospheric column, not layers within the cloud.

Page 3, line 6: Do you expect any diurnal cycle in the cloud properties that would mean that the derived statistics are not representative of the Arctic as a whole?

We did not investigate the diurnal cycle in the cloud properties. This is not possible since the radiosonde is most of the year only launched once per day (11 UTC). Since we do not expect any diurnal cycle, we consider the statistics as representative for the location as a whole. However we want to point out that there are differences in the weather at Ny-Ålesund compared to other locations in the Arctic due to the location in a fjord on the west coast of Svalbard compared to the typical sea ice influenced high Arctic. We consider Ny-Ålesund as an Arctic but not as a high Arctic location.

Page 3, line 10: I think data is plural, so it should be “data are” rather than “data is” We have changed it at page 3, line 10. At other places either only radiosonde or only radar is used in connection with data. Then it is grammatically correct to use “radar data is”.

Page 3, line 28: What statistical test was applied to show that the results did not change significantly?

No statistical test was applied. The use of the word significantly is wrong here. It is now changed to substantially.

Page 7, line 9: Why is only the lowermost 100 m considered?

We rephrased the sentence to make this more clear to ”For the subsaturated layer in between only the lowermost 100 m are evaluated in order to address the question if the ice crystal survives so far. If the layer is thinner than 100 m only the available vertical thickness is considered.” If there is no radar signal in this lowest part, then the ice crystal has not survived.

Page 10, line 11: Vali (200x?) has recommended that ice nucleating particles (INPs) rather than ice nuclei (IN) be used in order to standardize terminology. Recommend that you use INP rather than IN.

Thanks for the comment, we have changed it accordingly.

Page 15, line 1: The cloud layers can slope up and down frequently (in relatively short distances or times) and that can have a big impact on averaging. Was this taken into account?

The radar signal was averaged over a time of ± 30 min. Sometimes we have conditions like e.g. no cloud/high cloud at the start time (-30 min) and later (+30 min) a cloud reaching much lower (e.g. 3.7., 31.7., 18.8., 2.10., 14.2., 21.5.). In these cases the layer is almost half covered and half not covered and it is unclear if this should be counted as a cloud containing layer or not. Then averaging is the most consistent solution. Reducing the average time to ± 15 min does not improve the results, the Heidke skill scores are reduced in this case by 0.02 and 0.01.

Page 17, line 3: Perhaps I am not looking in the right place, but I cannot find the supplement being referred to in this statement.

You are completely right. This is now corrected.

References

- A. Korolev, G. Isaac, and J. Hallett. Ice particle habits in arctic clouds. *Geophysical research letters*, 26(9):1299–1302, 1999.
- M. Krämer, C. Schiller, A. Afchine, R. Bauer, I. Gensch, A. Mangold, S. Schlicht, N. Spelten, N. Sitnikov, S. Borrmann, et al. Ice supersaturations and cirrus cloud crystal numbers. *Atmospheric Chemistry and Physics*, 9(11):3505–3522, 2009.

- G. Mioche, O. Jourdan, J. Delanoë, C. Gourbeyre, G. Febvre, R. Dupuy, M. Monier, F. Szczap, A. Schwarzenboeck, and J.-F. Gayet. Vertical distribution of microphysical properties of Arctic springtime low-level mixed-phase clouds over the Greenland and Norwegian seas. *Atmospheric Chemistry and Physics*, 17:12845–12869, 2016.
- D. L. Mitchell. Use of mass-and area-dimensional power laws for determining precipitation particle terminal velocities. *Journal of the atmospheric sciences*, 53(12):1710–1723, 1996.
- T. Nomokonova, K. Ebell, U. Löhnert, M. Maturilli, C. Ritter, and E. O’Connor. Statistics on clouds and their relation to thermodynamic conditions at ny-ålesund using ground-based sensor synergy. *Atmospheric Chemistry and Physics Discussions*, 2018:1–37, 2018. doi: 10.5194/acp-2018-1144. URL <https://www.atmos-chem-phys-discuss.net/acp-2018-1144/>.
- M. Vassel, L. Ickes, M. Maturilli, and C. Hoose. Classification of Arctic multilayer clouds using radiosonde and radar data. *Atmospheric Chemistry and Physics Discussions*, 2018:1–22, 2018.
- J. Verlinde, J. Y. Harrington, V. Yannuzzi, A. Avramov, S. Greenberg, S. Richardson, C. Bahrmann, G. McFarquhar, G. Zhang, N. Johnson, et al. The mixed-phase Arctic cloud experiment. *Bulletin of the American Meteorological Society*, 88(2):205–221, 2007.
- J. Verlinde, M. P. Rambukkange, E. E. Clothiaux, G. M. McFarquhar, and E. W. Eloranta. Arctic multilayered, mixed-phase cloud processes revealed in millimeter-wave cloud radar Doppler spectra. *Journal of Geophysical Research: Atmospheres*, 118(23), 2013.
- C. D. Westbrook, R. J. Hogan, and A. J. Illingworth. The capacitance of pristine ice crystals and aggregate snowflakes. *Journal of the Atmospheric Sciences*, 65(1):206–219, 2008.

2 Answer to review 2

Interactive comment on “Classification of Arctic multilayer clouds using radiosonde and radar data” by Maiken Vassel et al.

Anonymous Referee #2

Received and published: 23 October 2018

We thank the anonymous reviewer for his/her review and the detailed comments. We have revised the manuscript accordingly, including a revision of all sublimation calculations, updates of all figures, and major changes of the text. Our replies to your comments are given below in blue after the specific comment. Our page references refer to the corrected version of the paper.

Summary of the manuscript

The study titled “Classification of Arctic multilayer clouds using radiosonde and radar data” by Maiken Vassel et al. describes an algorithm for the classification of multi-layer cloud occurrence for a one year dataset in Ny Alesund, Svalbard based on radiosonde and vertically-pointing cloud radar observations. The classification is two-fold: Firstly, only the conditions for cloud occurrence based on radiosonde humidity profiles consisting of two supersaturated layers separated by a subsaturated layer are analyzed. The fall distance of a hexagonal ice crystal of 100 micron size before complete evaporation in the subsaturated layer are estimated. The subsaturated layers are then classified into two categories. The first category is called “seeding”, referring to layers with a vertical extent lower than the fall distance before complete ice crystal sublimation. The second category is called “non-seeding”, referring to layers with a vertical extent higher than the fall distance before complete ice crystal sublimation. These maximum possible occurrence frequencies for multi-layer cloud occurrence based on supersaturated layers as identified by radiosonde ascents are then verified by cloud radar reflectivity profiles obtained within 30min before radiosonde launch and 30min after the radiosonde has reached 10 km altitude. Multilayer mixed-phase cloud occurrence was found in 29% of the cases based on the combined radiosonde-cloud radar estimation. One of the main findings of the paper is that about 50% of the multilayer clouds estimated solely from radiosonde humidity profiles are not classified as such by the radar. - But the conclusion that radiosounding data is not sufficient for multi-layer cloud occurrence classification since not only humidity but also concentrations of ice nucleating particle (INP) and cloud condensation nuclei (CCN) are crucial is not made.

We added an explanation of the missing overlap of radiosonde and radar data on page 11 by referring to Spichtinger et al. (2002): “In the ice-supersaturated layers above and below missing cloud formation can be explained by the lack of aerosol as INP (Spichtinger et al., 2002)”. Also in the conclusions we refer to this problem. Here we reworded the sentence to: “A high amount of supersaturated layers found in the radiosonde profiles does not coincide with observed cloud occurrence, probably due to lack of INP and thereby missing cloud formation” (page 17).

I would suggest the manuscript to be published after major revisions. The authors should address the following points:

Major comments:

The literature review in the introduction should be extended. For example: p.1 line 20: Some more recent publications on Arctic mixed-phase cloud properties should also be included, for example Shupe 2011 (DOI: 10.1175/2010JAMC2468.1). In this paper. e.g., the occurrence of mixed-phase clouds at Arctic sites was found up to altitudes of 7-8 km.

Thanks for the comment. We have corrected this and added the suggested reference.

p.2 line 18: Please give a broader and more detailed introduction on seeder-feeder mechanism and why it is important to consider it in the Arctic. Also, be more specific in which way the ice crystals falling from the upper cloud “influence” the lower cloud. Since this is a central question of this study, it has to be properly introduced. The points made in various parts of the manuscript (especially Section 2.3) need to be more precise instead of using colloquial expressions like “surviving” ice crystals etc. (e.g., also: p.6 line 24-29; p. 10 line 1-16, p.11, line 29-30, p.16 lines 18-20, etc.: very colloquial language).

We have added a more detailed description about the possible outcomes of the seeder-feeder mechanism (page 2, line 17 onwards). Regarding the use of the term *survive*, we have now defined it on p.4, l.21 and use it further on. In some passages we have exchanged *surviving* with *not fully sublimated* (e.g. section 2.3).

p.6 line 24-29: We have moved the sentence about the detection limit to the section 2.1.: “The detection limit is -19.47 dBZ at 223 m, -57.31 dBZ at 423 m and -28.61 dBZ at 10 km”.

p. 10 line 1-16: We have reworded the passage to: “For the seeding cases the cloud categories are shown in Fig. 8...” (p.10, l.21 - p.11, l.15).

p.11, line 29-30: We have changed it to: “A discontinuous radar signal only existing of small shreds of clouds is not counted as cloud and a continuous radar signal containing some small cloud free holes is counted as cloud.”

p.16 lines 18-20: We have changed it to: “Following from our sublimation calculation we find that MLCs, which are clearly (visibly) separated in the radar, do not interact through seeding. However, we have to keep uncertainties like the radar detection limit in mind.”

p.4 line 1-14: Please include a conceptual sketch of which kind of cloud layers you are considering indicating minimum depth of the layers, minimum vertical spacing between two supersaturated layers with a subsaturated layer between, temperature restrictions... otherwise it is really hard to follow.

On p.6 we have added a conceptual sketch of how we consider the radiosonde and radar data for potential MLCs.

p.4: It is mentioned that a simplified approach is used to determine the capacitance for a hexagonal plate. (By how much) does the capacitance differ for different ice crystal shape assumptions (columns/dendrites/quasi-spherical spheres)? Also, why do you use a radius-volume relation of a sphere (p.5) if you consider hexagonal plates? As e.g. shown by Mitchell, JAS 1996, ice particle fall speed is a strong function of ice particle shape and density. Only assuming one particular ice crystal shape (hexagonal plates) is not sufficient for the fall distance estimation. Sublimation calculations should at least be repeated for two other ice particle shapes with very different fall speed characteristics such as columns and dendrites which would lead to very different fall distances. Additionally, please mention the influence of up- and downdrafts on ice particle fall velocity and thus fall distance.

The first reviewer also commented on the ice crystal shape. We agree with you that the ice crystal shape should not be treated as a sphere. We changed the calculation and the text accordingly (p.4 and p.6). We have selected the four ice crystal shapes hexagonal plate, rimed particle, stellar and irregular particle which are representative for mixed-phase clouds (Mioche et al., 2016). For these particles we use the fall speed calculation shown in Fig. 1 and given by Mitchell (1996). We selected the particles to be realistic for both mixed-phase clouds and cirrus clouds. Additionally we chose the four shapes where the falls speeds varies the most. The main focus in the paper is on the hexagonal plate. The results for the other shapes is presented in the Appendix. We do not account for the lower limit of ice crystal size given by Mitchell (1996), since in our calculation we have to calculate the speed also for very small ice crystals due to sublimation. Note that this might lead to a small error of too fast falling small ice crystals.

We also corrected the capacitance. We are now using the calculation of Westbrook et al. (2008). The cases selected are listed on p.19 in the paper, as well as the aspect ratios chosen by us. In the last column the calculated capacitances for $r = 400 \mu\text{m}$ are shown. For the selected ice particle shapes the values range between $C = 2.00 \times 10^{-4}$ to $C = 3.88 \times 10^{-4}$. Earlier we used a capacitance of $C = 2.55 \times 10^{-4}$ for $r = 400 \mu\text{m}$.

We added a sentence pointing to the uncertainty due to the missing consideration of the up- and downdrafts.

In Fig. 2 we present the impact of the different ice crystal shapes on the result of classification step 2. As mentioned in the paper, for classification step 1 there is a small impact, but for classification step 2 there is almost no impact of the ice crystal shape on the result (p.10, l.4 and p.12, l.14-15).

p.6 line 24-29: Very colloquial language describing the radar reflectivity above the detection limit (p.6) - please rephrase. Please describe you averaging more in detail: I assume you refer to temporal averaging at each altitude? Please include a third Panel in Fig.2 showing the radar reflectivity sensitivity profile and the averaged reflectivity of the example case (for 50% data points within the considered time span).

We have reworded it in the text to "If more than 50 % of the selected radar data contain radar reflectivity factor data (coloured in Fig. 3b), then it is defined as cloud by the

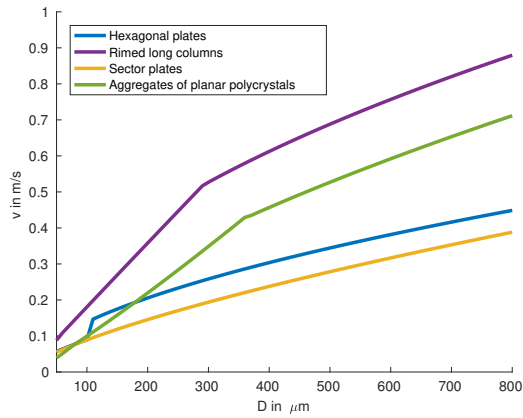


Figure 1: Ice crystal fall speed in dependence of particle size (Mitchell, 1996)

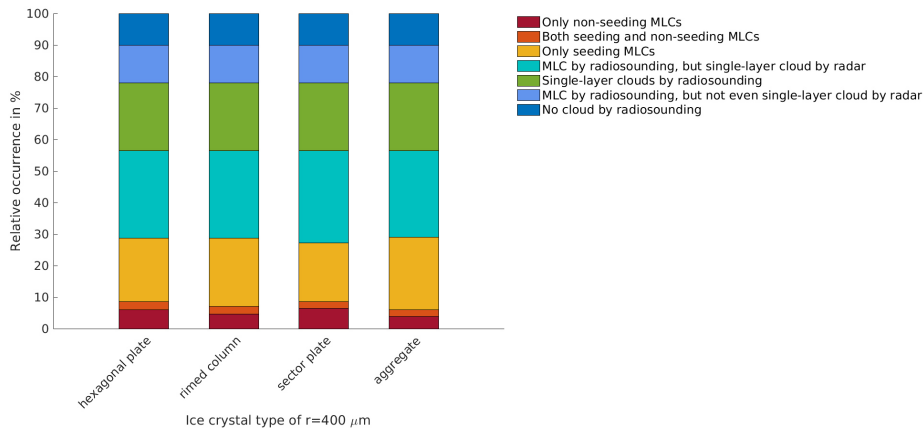


Figure 2: Classification step 2 using different ice crystal shapes with $r = 400 \mu\text{m}$.

algorithm” (p.8,1.6 onwards). We consider a box with 100 m height (see dashed boxes in Fig. 2 in the paper) and within this box we do not average but evaluate if more than 50% of the pixels contain radar reflectivity data. In Fig. 3 we show the radar sensitivity and the averaged reflectivity for each layer for the 3 November 2016. The measured reflectivity is above the radar sensitivity limit. On p.3 we added the sentence: ”The detection limit is -19.47 dBZ at 223 m, -57.31 dBZ at 423 m and -28.61 dBZ at 10 km, and the evaluated values are about these limits.“

p.8: I haven’t seen a definition for a cloud case – how long of a gap in time is needed to refer to a scene having two separate clouds at one altitude– one radar profile (30s?) or a few minutes? Or is this not considered at all and averaging over time around RS launch is done in a way that separate cloud occurrences at one height are averaged into “one”?

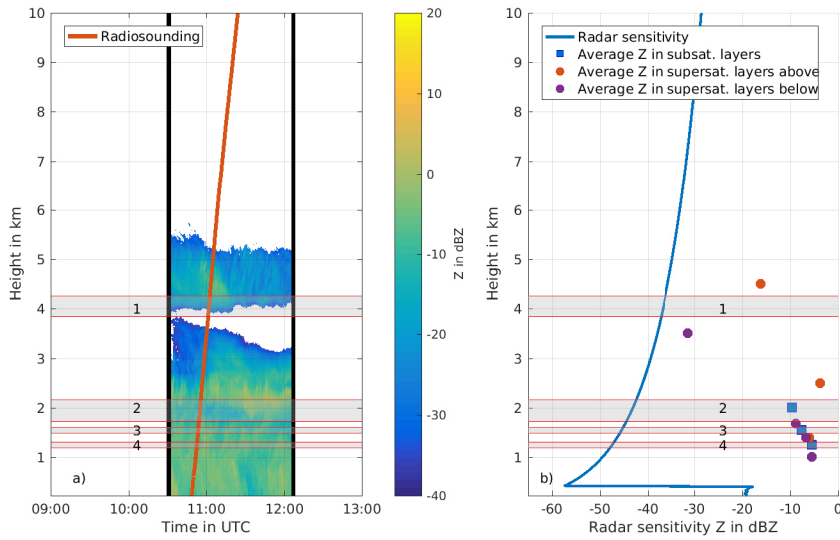


Figure 3: a) Radar reflectivity factor, b) Radar sensitivity: Minimum detectable radar reflectivity as a function of height. It includes the effect of ground clutter and gas attenuation but not liquid attenuation. The averaged reflectivity is shown for each layer.

Two clouds at one altitude are not considered separately. The evaluation over time is done so that separate clouds at the same altitude are considered as one cloud within this timespan (± 30 min).

p.10 lines 1-4: I do not fully agree with your conclusion that no cloud return in the radar data always means cloud-free conditions. There could be situations in which the sensitivity of the radar is not high enough (LWC and IWC too low). – I thus strongly suggest to also use available profiling lidar data (ceilometer) instead of only radar data to check for cloud occurrence in supersaturated conditions. Although the ceilometer suffers from full attenuation at sufficiently optically thick clouds, it will likely increase the number of detected cloud occurrences from ground-based remote sensing observations.

On p.11 we added the sentence: "Indeed, a very low liquid and ice water content could also result in a value below the radar sensitivity limit explaining these cases."

From 10.6.2016 onwards radar data was recorded in Ny-Ålesund and therefore we started our time period on this date. We would have liked to include micro-pulse lidar data as provided by https://mplnet.gsfc.nasa.gov/data?v=V2&s=Ny_Alesund&t=20160616, but this record ended at 16.06.2016. In Fig. 4b) we show the ceilometer attenuated backscatter coefficient for the 3 November 2016. It gives us the lowest cloud base height, but not any information on the additional cloud base heights above.

Moreover, in the Arctic frequently clouds occur at very low altitudes which might some-

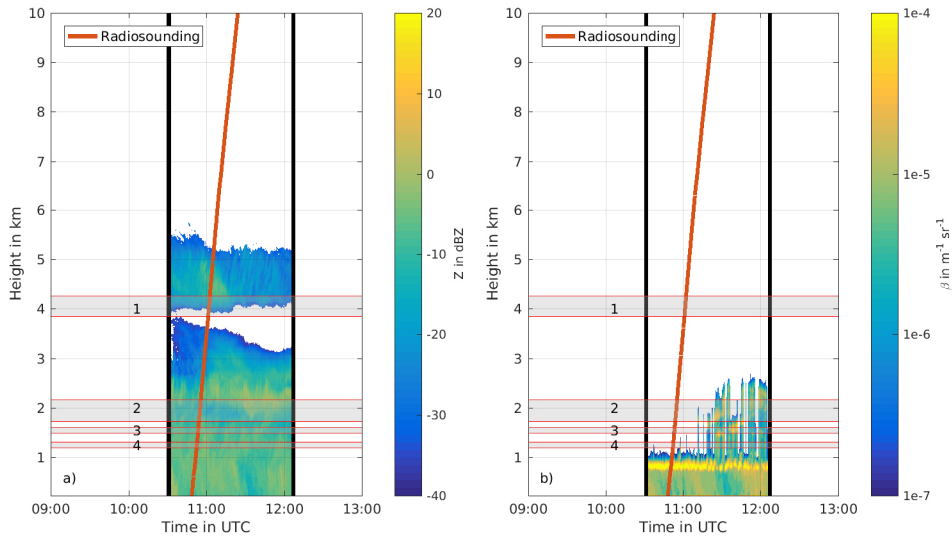


Figure 4: a) Radar reflectivity factor, b) Attenuated backscatter coefficient measured by Vaisala 910-nm CL51 lidar ceilometer in Ny-Ålesund

times be below the lowest radar/lidar range gate. On page 16 (line 15-16) you mention that a lidar would be useful. I strongly suggest making use of the existing ceilometer data (<https://www.awipev.eu/awipev-observatories/cloud-cover/>) in your study.

In the comment before we explained the problems when including the ceilometer. You are right, it is possible that we miss cloud layers existing only below 223 m. On p.3 we have added: "The detection height extend from 223 m until 10 km." and on p.11 we have added: "Additionally, the minimum detection height of 223 m might lead to some cases not considered." in order to point out that we might miss some cases. However, we have looked through this lowest layer in the relative humidity measurements and we do not think that there are many cases we miss.

Minor comments:

We have added all the following minor corrections.

Title: I suggest adding "in Svalbard" to narrow down the geographical range of the study. Also, since you are only considering $T < 0^{\circ}C$, you can add "cold" clouds in the title.

The new title is now: "Classification of Arctic multilayer clouds using radiosonde and radar data in Svalbard". We have added "in Svalbard" but we did not add "cold". We do not find this specification necessary. There is almost no case of MLC that we miss due to the temperature restriction $< 0^{\circ}C$.

p.4: For all variables in the equations the units should be included.

p.1 Line 10-13: It is unclear which kind of “deviations” you refer to – please specify more in detail.

We have changed the sentence to the following: “Since there are various deviations between the relative humidity profiles and the radar images, e.g. due to horizontal wind drift and time restriction, an evaluation by manual visual inspection is additionally done for the non-seeding cases.”

p.1 line 16: it should be “improve” instead of “improved”

p.1 line 16: hydrometeor shape and density (and thus terminal fall velocity) are of great importance, too.

p.1 line 21: You could add that the typical structure of stratiform mixed-phase cloud with supercooled liquid top layer and precipitating ice points to heterogeneous ice formation processes (add citation).

p.1 line 21: rather from the “remote sensing point of view”

p.1 line 22ff: “variable lidar signals inside a more or less continuous radar signal” sounds very imprecise – please rephrase and refer to “cloud profiles obtained with vertically-pointing instruments” or sth. similar

We have changed the sentence to: “From the remote sensing point of view, Verlinde et al. (2007, 2013) obtained cloud profiles with vertically-pointing instruments and described multilayered clouds as multiple distinct liquid layers within one vertical extensive cloud.”

p.1 line 24: make it easier for the reader and put multilayered vs. multilayer in Italics or bold font

p.1 line 24: In which measurement is the interstice of multilayer clouds visible – in profiles of radar or lidar or both?

In both lidar and radar measurements the interstice of multilayer clouds could be visible. However, since the lidar is usually not able to penetrate the lower cloud layer, we focus here on radar measurements.

p.2 line 2: I suppose, you mean “at least” two clouds in different heights since there can be very low boundary layer clouds, midlevel clouds, and high-level clouds occurring simultaneously

p.2 line 20: Please modify the sentence since you look at one specific Arctic site (... occur at Ny Alesund not “the Arctic”)

p.2 line 20: Why “thereby”?

We exchanged “Thereby we include...” with “We include...”

p.2 line 22: it should be “ground-based remote sensing” measurements

p.2 line 23: What do you mean by “easily accessible”?

Ground-based measurements are rare in the Arctic. Field campaigns are only limited to

a short time period. Radiosondings have the great advantage, that they are conducted all year around, each day and at multiple places all over the Arctic. In order to construct a classification, data availability over a full year is a great advantage. To compare various Arctic sites, the same type of measurement (radiosonde) is favourable.

p.2 line 25: be more precise in your wording: Instead of “radar” it should be profiling/zenith-pointing Doppler cloud radar

p.3 line 20: Please give a rough estimate of horizontal drift of the sondes based on their GPS tracking.

The first reviewer commented this as well. We present the same correction to both of you: In order to account for the horizontal drift, we calculate the wind speed in each layer. Using this information together with the distance between the radiosonde and the radar, we calculate the time at which the air parcel measured by the radiosonde was at the position of the radar. For this we do not consider the wind direction, but assume that the air parcel drifts the same direction as the radiosonde. As an example we show the results of the calculation for 3 November 2016 (Fig. 5). For the 3 November 2016 the average time over all heights is 12.94 min. For our statistics we add the average time for each day to the time chosen for the evaluation of the radar data. For the 3 November 2016 the resulting radar time period is shown in Fig. 6.

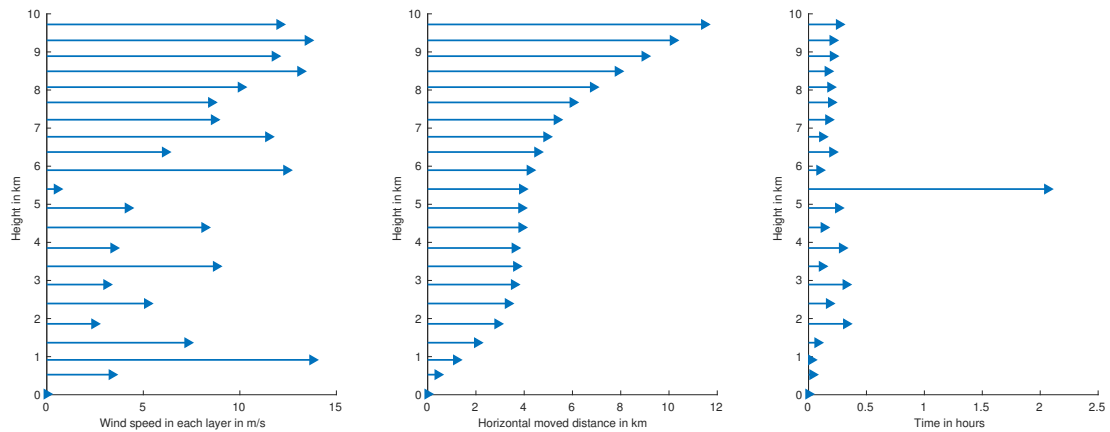


Figure 5: Advection on 3 November 2016: a) windspeed in each height layer, b) distance between radar and radiosonde, c) time the air parcel needs to drift from the radar to the position of the radiosonde.

p.3 line 23: Please also indicate the lowest radar range gate and mention that the cloud Doppler radar is zenith-pointing. You mention a vertical radar range gate resolution of 20m, is it really the same at all altitudes (i.e., all chirps) and was the RPG radar really operated in the same mode (with the same vertical and temporal resolution) over the entire year? 30s temporal resolution seems very low – please verify this temporal resolution... or are you using data already averaged to Cloudnet temporal resolution?

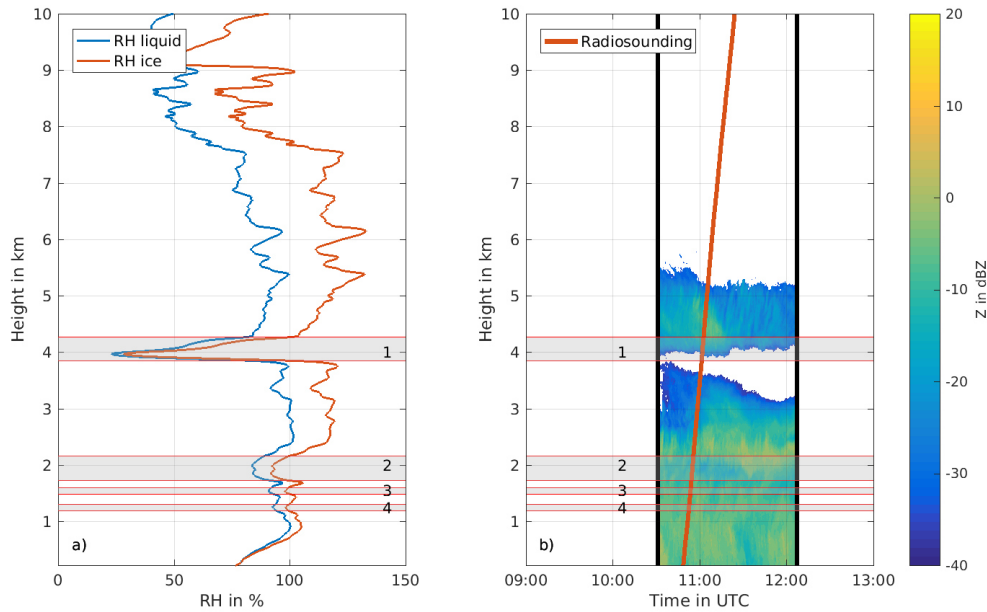


Figure 6: a) Radiosonde data, b) radar time period corrected due to advection. At the time when the radiosonde reached the supersaturated layer 1 at 3.85 km the radiosonde is 3.70 km away from the radar due to horizontal wind drift.

You are right, we use data already averaged to Cloudnet resolution. That is why our data has a vertical resolution of 20 m at all heights and a temporal resolution of 30 s. The lowest range gate provided in our data set is 223 m. We have highlighted in the text that we use the averaged data. The original resolutions are different: The radar was operated in the high resolution mode. Here the vertical resolution varies from 4 m at 100 m height to 17 m at 10 km. The lowest range gate measured by the radar is 100 m. The temporal resolution is continuously 2.5 s.

p.3 line 25: Please indicate typical values of attenuation correction for the 94GHz radar at Ny Alesund.

Typical values of two-way radar attenuation due to atmospheric gases are between 0.09 dB at 223 m height and 1.20 dB at 10 km height (Fig. 7).

p.3 line 25: What do you mean by “at all frequencies”?

We have deleted “by all frequencies”. It was formulated in this way as calibration convention in the data description, but for this specific radar there is only one frequency.

p.6 line 4: ice crystal size r refers to maximum dimension? Motivate the choices of ice crystal size of 50/100/150 microns by citing typical values found in Arctic clouds.

Already the first reviewer commented this. We present the same correction and answer to both of you: This is a valid comment, and we have revised the calculations taking into account larger crystal sizes. The upper cloud of a MLC, from where the falling

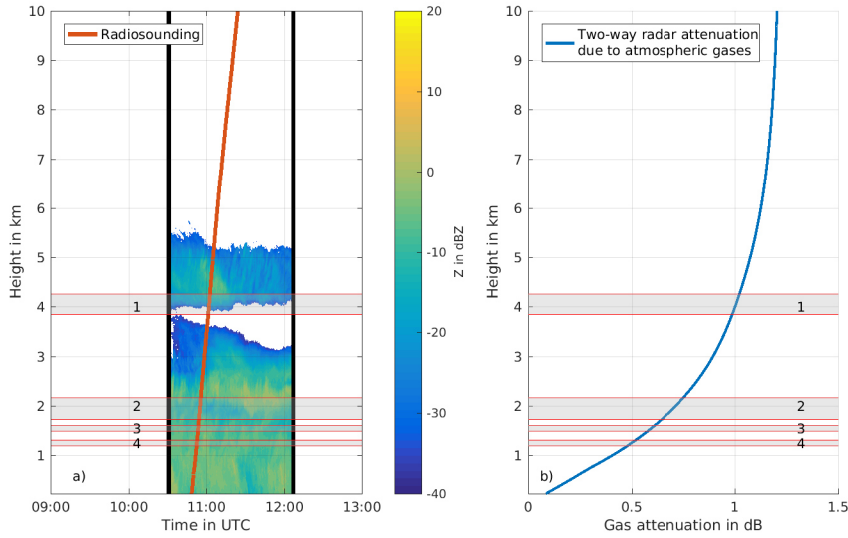


Figure 7: a) Radar reflectivity factor, b) Two-way radar attenuation due to atmospheric gases used for correcting Z .

ice crystals origin, can either be a mixed-phase cloud or a cirrus cloud. In mixed-phase clouds Korolev et al. (1999) measured ice crystals with radii of about $r = 400 \mu\text{m}$. We also refer to Fig. 5e in Mioche et al. (2016), where a radius of $r = 400 - 500 \mu\text{m}$ can occur in mixed-phase clouds. For cirrus clouds Krämer et al. (2009) showed that the radii of ice crystals range between $r = 1 - 100 \mu\text{m}$. In order to account for both cloud types, we have redone our calculations for the ice crystal sizes $r = 100, 200$ and $400 \mu\text{m}$. Our main focus is now on $r = 400 \mu\text{m}$, assuming in most cases the upper cloud to be mixed-phase. With r we refer to the maximum dimension, $r = D_{\text{max}}/2$.

p.6 line 4: It is unclear what you mean by “mean conditions”: Mean over one hour after radiosonde launch?

By mean conditions we mean the average of the variable (pressure, temperature, humidity) over the height levels of the specific subsaturated layer.

p.6 line 5: “survive” is very colloquial, please replace or describe what you mean. Please change accordingly throughout the text.

We have now defined seeding on p.4, l.20 and use it therefore in the following text. In some passages we have exchanged *surviving* with *not fully sublimated* (e.g. p.6 l.11).

p.6 line 17: The way it is presented it sounds like as if the radar is used to test for cloud occurrence (above/between/below) in general and not only for cloud occurrence in general (Also see Table 1). (?)

We have corrected the sentence to: “The aim of adding radar data to the classification is

to cross-check the super- and subsaturated layers in the radiosonde profiles with actual cloud occurrence.”

p.6 line 19-20: Clarify why you use 30min after the radiosonde reached 10km as end time and not e.g. simply a one hour time around RS launch (start 30min before and end 30min after launch)?

If we simply use a one hour time slot around the radiosonde launch start, we have cases (30.6.16) where in the height levels above 8 km the averaging of the radar data ends before the launched radiosonde reaches this height level. In order to avoid this we use + 30min after the radiosonde reached 10km as end time.

p.6 line 29-30: “Evaluated” in which way?

We have changed it to: “For the *subsaturated layer in between* only the lowermost 100 m are analysed in order to address the question if the ice crystal survives so far.”

p.6 line 31: 50% of what? Of all pixel within a 100m x time from RS launch to 30min after RS end? Or 50% of pixel at a certain altitude?

We mean the 50% data points in the area of 100 m x time from RS launch (- 30min + advection time) to RS end (+ 30min + advection time).

p.6 line 34: Specify that the ice crystal is actually growing in the supersaturated layer and which microphysical growth processes could occur and specify in which way the ice crystal can “influence” the cloud.

We have changed it to: “The ice crystal begins to grow and can influence a cloud no matter at which height it is within the supersaturated layer.” Further details on the influence of additional ice crystals on the cloud is mentioned when explaining the seeder-feeder effect (p.2,1.16-26).

p.7 line 12 -13: Why do you refer to seeding situations here when you describe non-seeding situations in line 10-11?

We have resorted and reformulated the sentences. We want to point out which two cloud categories we have chosen to be MLC cases (one non-seeding and one seeding case).

p.9 line 8-10: Describe the influence of varying ice crystal size more in detail: 57% of possible seeding for 150micron ice particle size and only 37% for 50micron...

We reworded it at p.10, 1.6-1.12.

p.9 line 11: Please expand your discussion of Figure 5. In number indicate the number of cases considered for each month (February maybe has a much lower number of cases?).

We have added the number of cases (days) to Fig 5. You are right, during February there are less analysed days. This is due to the lack of radar data during this month. We reworded and expanded section 3.1.

p.10 line 2: Define acronym IN(P)

We already defined INP on page 2.

p.16 line 2: vertically-pointing cloud Doppler radar (instead of only “radar”)

References

Korolev, A., Isaac, G., and Hallett, J.: Ice particle habits in Arctic clouds, *Geophysical research letters*, 26, 1299–1302, 1999.

Krämer, M., Schiller, C., Afchine, A., Bauer, R., Gensch, I., Mangold, A., Schlicht, S., Spelten, N., Sitnikov, N., Borrmann, S., et al.: Ice supersaturations and cirrus cloud crystal numbers, *Atmospheric Chemistry and Physics*, 9, 3505–3522, 2009.

Mioche, G., Jourdan, O., Delanoë, J., Gourbeyre, C., Febvre, G., Dupuy, R., Monier, M., Szczap, F., Schwarzenboeck, A., and Gayet, J.-F.: Vertical distribution of microphysical properties of Arctic springtime low-level mixed-phase clouds over the Greenland and Norwegian seas, *Atmospheric Chemistry and Physics*, 17, 12 845–12 869, 2016.

Mitchell, D. L.: Use of mass-and area-dimensional power laws for determining precipitation particle terminal velocities, *Journal of the atmospheric sciences*, 53, 1710–1723, 1996.

Spichtinger, P., Gierens, K., and Read, W.: The statistical distribution law of relative humidity in the global tropopause region, *Meteorologische Zeitschrift*, 11, 83–88, 2002.

Westbrook, C. D., Hogan, R. J., and Illingworth, A. J.: The capacitance of pristine ice crystals and aggregate snowflakes, *Journal of the Atmospheric Sciences*, 65, 206–219, 2008.

3 List of all relevant changes

See review answers and marked-up manuscript version for list of all relevant changes made in the manuscript.

4 Marked-up manuscript version

Classification of Arctic multilayer clouds using radiosonde and radar data in Svalbard

Maiken Vassel¹, Luisa Ickes², Marion Maturilli³, and Corinna Hoose¹

¹Institute of Meteorology and Climate Research, Karlsruhe Institute of Technology, Karlsruhe, Germany

²Department of Meteorology, Stockholm University, Stockholm, Sweden

³Alfred Wegener Institute for Polar and Marine Research, Potsdam, Germany

Correspondence: Maiken Vassel (maiken.vassel@alumni.kit.edu), Luisa Ickes (luisa.ickes@misu.su.se)

Abstract. Multilayer clouds (MLC) occur more often in the Arctic than globally. In this study we present the results of a detection algorithm applied to radiosondes and radar from an one-year time period in Ny-Ålesund, Svalbard. Multilayer cloud occurrence ~~was-is~~ found on 29 % of the investigated days. These multilayer cloud cases are further analysed regarding the possibility of ice crystal seeding, meaning that an ice crystal can survive sublimation in a subsaturated layer between two cloud layers when falling through this layer. For this we analyse profiles of relative humidity with respect to ice to identify super- and subsaturated air layers. Then the sublimation of an ice crystal of an assumed initial size of ~~$r = 100 \mu\text{m}$~~ $r = 400 \mu\text{m}$ on its way through the subsaturated layer is calculated. If the ice crystal still exists when reaching a lower supersaturated layer, ice crystal seeding can potentially take place. Seeding cases are found often, in 23 % of the investigated days (100 % includes all days, also non-cloudy days). The identification of seeding cases is limited by the radar signal inside the subsaturated layer.

Clearly separated multilayer clouds, defined by a clear interstice in the radar image, do not interact through seeding (9 % of the investigated days). Since there are various deviations between the relative humidity profiles and the radar images, ~~for the non-seeding cases e.g. due to horizontal wind drift and time restriction~~, an evaluation by manual visual inspection is additionally done for the non-seeding cases.

1 Introduction

Clouds radiate downwards in the long-wave part of the spectrum and thereby warm the surface in the Arctic during most of the year (Shupe and Intrieri, 2004). However, the correct representation of cloud fraction, cloud water content and its phase, particle size, shape, density and cloud temperature is difficult but essential to ~~improved-improve~~ weather forecasting (Barrett et al., 2017a, b). Therefore clouds are still a major contributor to uncertainty in both weather and climate prediction.

In the recent years, an emphasis of research has been on Arctic mixed-phase clouds (Andronache, 2018; Morrison et al., 2012; Loewe et al., 2017). These clouds occur frequently in the Arctic, at all heights up to ~~6.5~~ 8 km, and exist in the temperature range between -34°C to 0°C (~~Intrieri et al., 2002~~)(Shupe, 2011; Intrieri et al., 2002). They often consist of a supercooled liquid layer at cloud top and precipitating ice particles below, which points to heterogeneous ice formation (Whale, 2018). From the ~~measurement-remote sensing~~ point of view, Verlinde et al. (2007, 2013) ~~described-multilayered-clouds-as-layers-of-variable-lidar (light-detection-and-ranging)-signals-inside-a-more-or-less-continuous-radar (radio-detection-and-ranging)~~

signal. ~~With that they refer to~~ obtained cloud profiles with vertically-pointing instruments and described *multilayered* clouds as multiple distinct liquid layers within one vertical extensive cloud. In contrast to ~~multilayered clouds, multilayer~~ multilayered clouds, *multilayer* clouds (MLCs) are described as two separate clouds with a clear visible interstice in between (Tsay and Jayaweera, 1984; Intrieri et al., 2002; Khvorostyanov et al., 2001; Fleishauer et al., 2002; Liu et al., 2012). The coexistence of at least two clouds in different heights, in the Arctic often a boundary layer cloud and a higher mixed-phase or cirrus cloud, can be explained by horizontally inhomogeneous advection (Luo et al., 2008). When large-scale meridional transport brings warm moist air into the Arctic, temperature and humidity inversions occur frequently (Nygård et al., 2014). Reaching supersaturation and in the presence of sufficient cloud condensation nuclei (CCN) and ice ~~nuclei~~ (IN)nucleating particles (INPs), this horizontal advection can result in cloud formation at multiple heights (Curry and Herman, 1985).

Christensen et al. (2013) analysed radar and lidar data collected by the satellites CloudSat (millimetre wavelength cloud profiling radar) and CALIPSO (Cloud–Aerosol Lidar and Infrared Pathfinder Satellite Observations) to investigate the occurrence of MLCs. They found, excluding the Arctic, the global average occurrence of MLCs to be 11 % of the data. For the Arctic, Liu et al. (2012) analysed similar satellite data of CloudSat and CALIPSO and found Arctic MLCs to occur between 17-25 % of the investigated time. The contribution of the MLCs to the seasonal variation of Arctic cloud coverage is only very weak. Cloud detection by satellites is challenging in the Arctic. A poor thermal and visible contrast between clouds and the underlying surface of snow and ice and small radiative fluxes from the cold polar atmosphere are only some of the uncertainties (Liu et al., 2012). Therefore and since the minimum considered layer thickness for separation was 960 m, Liu et al. (2012) assumed their estimated MLC occurrence most likely to be underestimated.

Microphysical interaction between MLC layers can happen through the seeder-feeder mechanism (~~Fleishauer et al., 2002; Avramov and~~ Fleishauer et al., 2002; Avramov and Harrington, 2010; Hobbs and Rangno, 1998; Houze Jr, 1993). This means that falling ice crystals from the upper cloud ~~influence the lower cloud. However, ice~~ enrich the lower cloud by additional ice crystals having an influence on the evolution of the phase of the lower cloud (e.g. glaciation). Vapour deposit at these ice crystals inside the lower cloud and the ice crystals grow. At the same time in the case of ice-supersaturation but liquid-subsaturation liquid water is depleted (Bergeron-Wegener-Findeisen process, Korolev (2007)). In the case of ice-supersaturation and water-supersaturation existing liquid drops compete for the water vapour with the ice crystals. Both the liquid and ice grow and the cloud strengthens. Depending on what kind of regime exists, both precipitation formation and cloud dissipation as well as cloud thickening are possible outcomes. However, if the fall speed of the ice crystals is large, then the time the ice crystals spend in the cloud layer is too short and no influence is also a possible outcome. However, ice formation in Arctic boundary layer clouds is not fully understood (Fridlind et al., 2012; Paukert and Hoose, 2014) and the frequency of seeding ice crystals from above into the lower cloud still needs to be investigated.

The objective of this study is to answer how often MLCs occur ~~in the Arctic. Thereby we at Ny-Ålesund, Svalbard. We~~ include an estimate for the possibility of the seeder-feeder mechanism between MLCs. For answering this question we present a MLC classification based on ground-based remote sensing and in-situ measurements. In this study the first step is the analysis of radiosonde profiles to estimate the presence of MLCs. Radiosondes have the advantage to be relatively easy accessible in the Arctic. In this way the algorithm for MLC detection could easily also be applied to various other Arctic locations. However,

the use of only radiosondes has limitations and needs to be verified. For this we chose Ny-Ålesund, ~~Svalbard~~, as an example study site where also [profiling / zenith-pointing Doppler cloud](#) radar data is available.

In Section 2 we present the datasets of radiosondes and radar used for the classification, we explain the methodology of the classification, and we consider the possibility of the seeder-feeder mechanism. In Section 3 we separate the results of the classification in seeding and non-seeding cases and compare them to a very simple visual detection. We present our conclusions of this study in Sect. 4.

2 Methodology of the Arctic MLC classification algorithm

2.1 Datasets

Ny-Ålesund is located along a fjord on the west coast of the Arctic archipelago Svalbard (78.9 °N, 11.9 °E). Due to its location in the North Atlantic region of the Arctic, clouds above Ny-Ålesund are not only influenced by typical high-Arctic stable weather conditions but are also frequently connected with cyclonic systems, as well as influenced by the mountainous orography of the archipelago. The occurring clouds might therefore differ from other Arctic sites, especially those over the pack ice. However, due to the good access to a one-year dataset of both radiosonde profiles and radar, it is a suitable choice for the evaluation of the detection algorithm.

For the classification radiosonde profiles and radar data from Ny-Ålesund between 10 June 2016 - 9 June 2017 are analysed. Out of this 1-year period we analyse 278 days when both radiosonde and radar data ~~is~~ [are](#) available. We consider the height range between 0 and 10 km. For each day, only the time frame of one hour after the radiosonde launch was considered. The regular launch time for the Ny-Ålesund radiosondes is 11 UTC. During campaign periods (e.g. 5 - 20 December 2016), additional launches at 5, 17, and 23 UTC are available. Within the analysed 1-year period, the station has changed the operational radiosonde type from Vaisala RS92 (until 11 April 2017) to Vaisala RS41 (from 12 April 2017), respectively. The humidity sensor of the RS92 (RS92, 2013) has a manufacturer given uncertainty of 5% and a response time of < 0.5 s to < 20 s (for + 20 °C to - 40 °C, 6 ms⁻¹, 1000 hPa), while the RS41 (RS41, 2017) is described with an uncertainty of 4% and a response time of < 0.3 s to < 10 s (for + 20 °C to - 40 °C, 6 ms⁻¹, 1000 hPa), respectively. The radiosonde data with 1 s resolution were applied from Sommer et al. (2012) for the RS92 period, and from Maturilli (2017) for the RS41 period. All radiosondes were launched on balloons with an ascent rate of approximately 5 ms⁻¹. The horizontal drift of the sondes depends on the atmospheric wind conditions.

A [zenith-pointing](#) 94-GHz Doppler radar has been operated in Ny-Ålesund since 10 June 2016 by the University of Cologne as part of the (AC)³ project ("Arctic Amplification: Climate Relevant Atmospheric and Surface Processes and Feedback Mechanisms"; Wendisch et al. (2017)). ~~The vertical resolution~~ [A detailed description](#) of the radar is [found in Küchler et al. \(2017\)](#). ~~We use averaged data having a vertical resolution of 20 m and it reaches up to a maximum height of 12 . The radar measures continuously with a~~ temporal resolution of 30 s. ~~A detailed description is found in Küchler et al. (2017)~~ [The detection height extends from 223 m until 10 km](#). The radar reflectivity factor was corrected for gaseous attenuation and the calibration was done in the way that a cloud at 273 K containing $1 \times 10^{-6} \text{ m}^{-3}$ droplets of $D = 100 \text{ }\mu\text{m}$ has a reflectivity factor of 0 dBZ.

The detection limit is -19.47 dBZ at 223 m, -57.31 dBZ at all frequencies-423 m and -28.61 dBZ at 10 km, and the evaluated values are above these limits.

For the cloud classification as step 1, radiosonde profiles are analysed regarding ice-supersaturation and ice-subsaturation. Secondly, as step 2, radar data is included in order to verify the MLC occurrence in these super- and subsaturated layers.

5 2.2 Classification step 1: Potential MLCs and sublimation calculation based on radiosonde profiles

The classification is divided into a step 1 and a step 2, as illustrated in Fig. 1. In step 1 we identify ice super- and ice subsaturated layers in the radiosonde profiles and calculate if ice crystal seeding is possible between these layers. We use the relative humidity with respect to liquid water from the radiosonde profile in combination with the temperature measurement and the formula of Hyland and Wexler (1983) to calculate the relative humidity with respect to ice. A sensitivity study where measurement uncertainties are accounted for by also considering the relative humidity $\pm 5\%$ is shown in Appendix Fig. A2 and Fig. A3. Super- and subsaturated layers are identified using a threshold of 100 % relative humidity with respect to ice. The same threshold was also chosen by Treffeisen et al. (2007). When using a different threshold, e.g. 120 %, the results do not change significantly substantially. If the temperature at certain levels is above 0 °C, then relative humidity with respect to water is chosen for limiting the subsaturated layer. Numerous very thin super- and subsaturated layers (< 100 m) exist in the radiosonde profiles, but these layers are too thin to be considered a relevant contribution to the described processes. In order to sort out some of these irrelevant layers, but also to include thin cloud layers (Luo et al., 2008), the minimum thickness limits for the supersaturated and subsaturated layers are set to 100 m. This is in close agreement to Verlinde et al. (2007) finding layers to vary between 50 m to 300 m in depth. In order to detect a potential MLC, the criteria of detection is one *subsaturated layer in between* (in the following termed cloudfree layer) one *supersaturated layer just above* (cloud layer) and one *supersaturated layer just below* (cloud layer)-, as illustrated in Fig. 2. Subsaturated layers between two supersaturated layers at temperatures above 0 °C are not considered, as they are not relevant for our main point of focus, ice crystal seeding. Note that this means that we might underestimate the amount of multilayer clouds. If there is no supersaturated layer or only one single supersaturated layer, then these cases are not considered further for MLC detection (dark blue and green case in Fig. 1).

In the next step the sublimation calculation is done in order to answer if a falling ice crystal could survive would not fully sublimate (hereafter "survive") on its path through the subsaturated layer. For this the equation of vapour deposition is used to calculate the reduction of ice crystal mass due to sublimation (ice to vapour),

$$\frac{dm}{dt} = 4\pi C \rho_i G_i s_i \quad (1)$$

$$G_i = \left[\frac{\rho_i RT}{M_w D_v e_i} + \frac{\rho_i l_s}{M_w k_T T} \left(\frac{l_s}{RT} - 1 \right) \right]^{-1} \quad (2)$$

m is the mass of one ice crystal and *C* is its capacitance (Lamb and Verlinde, 2011). The capacitance replaces the radius *r* of a liquid sphere and takes the shape of the ice crystal into account. A simplified approach is to use $C = \pi/2 \cdot r$ for a hexagonal plate (??). ρ_i is the density of ice, G_i the growth parameter and s_i the supersaturation regarding ice, which is given by

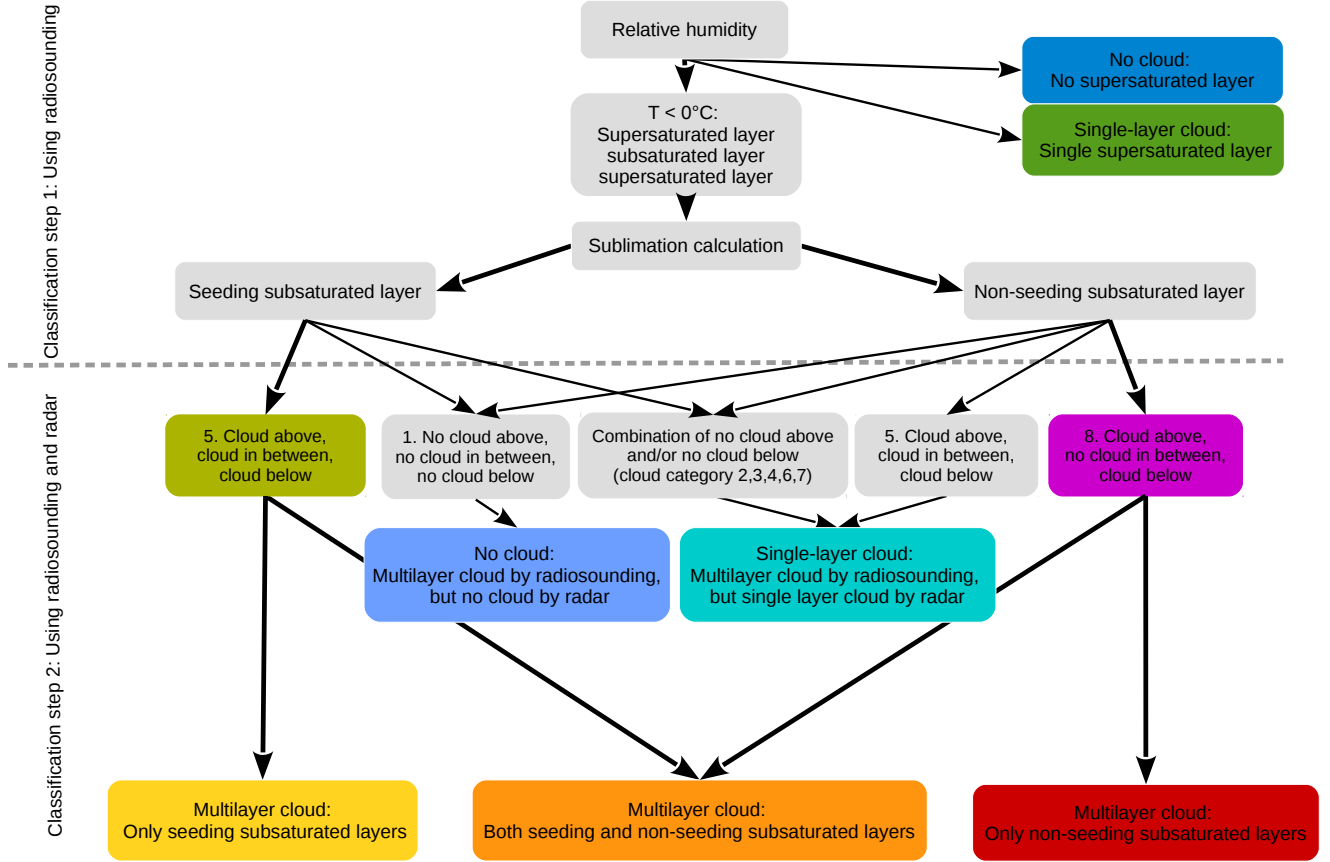


Figure 1. Overview of classification schemes: First only radiosonde data is used to detect one *subsaturated layer in between* two supersaturated layers, one just *above* and one just *below*. If this combination is found, then for the subsaturated layer the calculation of sublimation leads to seeding or non-seeding cases. Liquid layers above 0 °C are not considered. In the next step radar reflectivity factor data is added in order to detect cloud occurrence inside the investigated *supersaturated layer above* (*cloud above*), *subsaturated layer in between* (*cloud in between*) and *supersaturated layer below* (*cloud below*). The cloud category 5 ‘cloud above, cloud in between, cloud below’ is counted as seeding MLC since it is most likely the seeding resulting in a radar signal in the subsaturated layer in between the cloud layers. The colours yellow, orange and red represent the resulting MLC categories.

m is the mass in kg of one ice crystal and C is its capacitance in m (Lamb and Verlinde, 2011). The capacitance replaces the radius r of a liquid sphere and takes the shape of the ice crystal into account. In mixed-phase clouds Mioche et al. (2016) found mostly hexagonal plates, rimed particles, stellars and irregular particles. Our main focus is on the hexagonal plates, but by including this variety we cover the most usual shapes detected in both mixed-phase clouds and also cirrus clouds (Mioche et al., 2016; Mitchell, 1994). The calculation of the capacitance is based on Westbrook et al. (2008) and details are listed in A1. ρ_i is the density of ice in kg m^{-3} , G_i the growth parameter and s_i the supersaturation regarding ice, which is given by

$$s_i = \frac{e_i}{e_{\text{sat},i}(T)} - 1$$

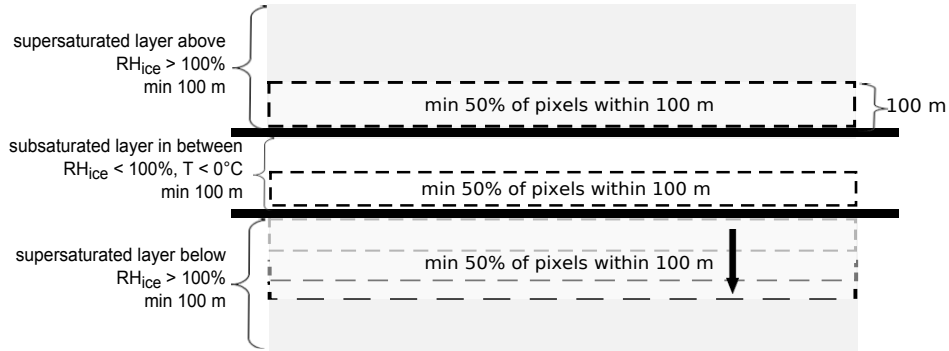


Figure 2. Conceptual sketch of criteria how potential MLCs are identified. The grey areas symbolise the supersaturated layers, in between the black lines is the subsaturated layer. The dashed boxes symbolise the areas within it is searched for cloud occurrence. In the supersaturated layer below it is first searched for cloud occurrence within a box close to top (dashed light grey), secondly the box is moved lower down (dashed medium grey and black).

and relates the actual ice saturation e_i to ice equilibrium saturation at a given temperature $e_{\text{sat},i}(T)$. In the case of subsaturation, the supersaturation is less than 0. Further variables in equation 2 are the temperature T , the heat transport k_T , the latent heat of sublimation l_s , the universal gas constant R , the molecular mass of water M_w and the diffusion coefficient D_v . D_v is in and is calculated using

and relates the actual ice saturation e_i in Pa to ice equilibrium saturation in Pa at a given temperature $e_{\text{sat},i}(T)$. In the case of subsaturation, s_i is less than 0. Further variables in equation 2 are the temperature T in K, the heat transport k_T in $\text{J m}^{-1} \text{s}^{-1} \text{K}^{-1}$, the latent heat of sublimation l_s in J mol^{-1} , the universal gas constant R in $\text{J kg}^{-1} \text{mol}^{-1}$, the molecular mass of water M_w in kg mol^{-1} and the diffusion coefficient D_v . D_v is in $\text{m}^2 \text{s}^{-1}$ and is calculated using

$$D_v = 0.211 \left(\frac{T}{T_0} \right)^{1.94} \frac{p_0}{p} \cdot 1 \times 10^{-4} \quad (4)$$

with $T_0 = 273.15$ and $p_0 = 1013.25$ (Hall and Pruppacher, 1976). By using equation 1 the change of mass dm with time dt is obtained. In addition to that, assuming the radius-volume relation of a sphere by using $V = m/\rho_i$, a new radius is obtained at each time step by $r = \sqrt[3]{\frac{3V}{4\pi}}$. In order to answer the question if an ice crystal could reach the lower supersaturated layer, the mass, reduced due to sublimation, at each time step is combined with a fall speed in order to yield a fall distance. For this the fall speed $v(m)$ parametrisation of ?

$$5 \quad v(\quad) \quad (5)$$

with $T_0 = 273.15$ K and $p_0 = 1013.25$ Pa (Hall and Pruppacher, 1976). By using equation 1 the change of mass dm with time dt in s is obtained. Based on Mitchell (1996), but here in SI-units, we use the mass-diameter relation

$$m) \cong \alpha \cdot \underline{m} \times 10^{-3} (d \times 10^2)^\beta, \quad (6)$$

with the diameter d in m and obtain a new radius at each time step. The parameters α and β depend on the ice crystal shape and are given by Mitchell (1996). For the calculation we use the hexagonal plates, rimed long columns, crystal with sector-like branches, and assemblages of planar polycrystals provided by Mitchell (1996). In order to answer the question if these ice crystals could reach the lower supersaturated layer, the mass, reduced due to sublimation, at each time step is combined with a fall speed in order to yield a fall distance. The fall speed v in ms^{-1} is provided by Mitchell (1996), here in SI-units, by

$$v = 1 \times 10^2 \cdot a \cdot \nu \left(\frac{\rho_{\text{air},0}}{\rho_{\text{air}}} \frac{2ag}{\rho_{\text{air}} \nu^2 \gamma \cdot 1 \times 10^3} \right)^{\gamma^b (d \times 10^2)^{b(\beta+2-\sigma)-1}}. \quad (7)$$

5 is used. Here are $\alpha = 0.217$, $\beta = 0.363$, $\gamma = 1/2$ empiric constants for cloud ice (hexagonal plates) and $\rho_{\text{air},0}$ is 1.225. The parameters γ and σ depend on the ice crystal shape and also a and b are given by Mitchell (1996). The air density ρ_{air} in kgm^{-3} is given by $\rho_{\text{air}} = p / (R_s \cdot T)$, where p is the actual pressure and R_s is the specific gas constant of air. g is the gravity in ms^{-2} and ν is the kinematic viscosity given by $\nu = \mu / \rho_{\text{air}}$, with μ being the dynamic viscosity. The calculation is done using the forward Euler method and a time step of 0.01 s. The initial ice crystal size is assumed to be $r = 100400$ μm ,
 10 but also $r = 50100$ μm and $150-r = 200$ μm are evaluated in order to account for both mixed-phase and cirrus clouds (Mioche et al., 2016; Krämer et al., 2009). Mean conditions of pressure, temperature and humidity of each analysed subsaturated layer are used. We do not take up- and downdrafts influencing the fall velocity into account. If the ice crystal survives is not fully sublimated until the lower supersaturated layer, then it is called a **seeding** subsaturated layer. A **non-seeding** subsaturated layer means that the given ice crystal does not reach the lower next supersaturated layer because it sublimates
 15 completely.

As an example for the classification we show the classification for the case on 3 November 2016 in Fig. 3a. There are four subsaturated layers regarding ice and these are indicated by red horizontal lines. For the subsaturated layer 1 between 4.26 km and 3.85 km height the sublimation calculation is shown in Fig. 4. In Fig. 4a the change of mass and the calculated fall speed is shown and in Fig. 4b the resulting fall distance inside the subsaturated layer 1 is shown. An ice crystal of initial
 20 size $r = 100400$ μm will sublimate completely before reaching the lower supersaturated layer and therefore the subsaturated layer 1 is a non-seeding one (red line in Fig. 4b). In the case of $r = 150$ the subsaturated layer 1 would be a seeding case. In the subsaturated In the subsaturated layers 2, 3 and 4 an ice crystal of initial size $r = 100400$ μm will survive not be fully sublimated and these layers are therefore determined as seeding layers (sublimation calculation not shown).

2.3 Classification step 2: Cloud occurrence based on radiosonde profiles and radar

25 The aim of adding radar data to the classification is to cross-check the super- and subsaturated layers in the radiosonde profiles with actual cloud occurrence. We use the radar reflectivity factor Z from the Doppler zenith-pointing Doppler cloud radar in

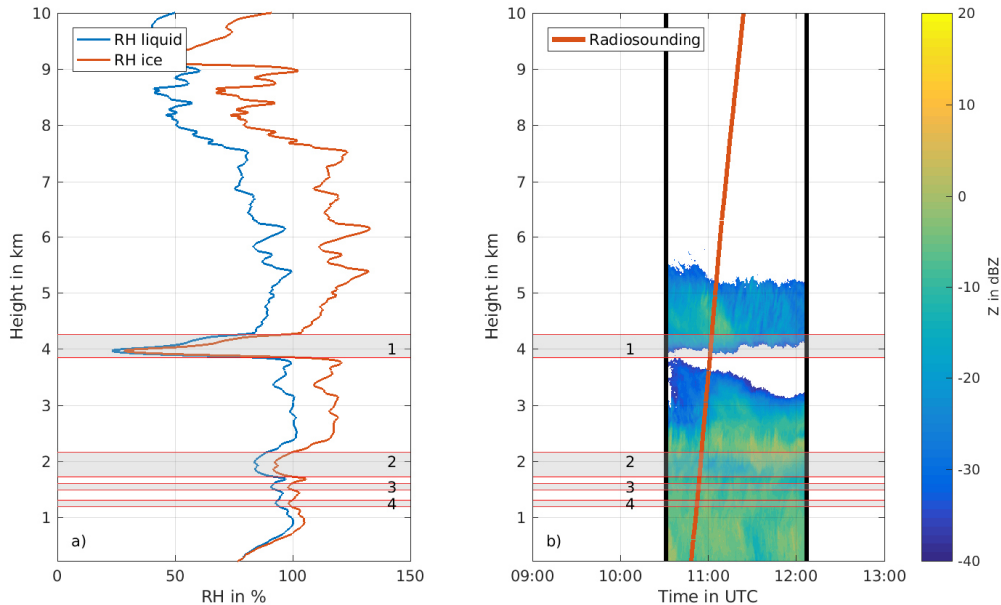


Figure 3. 3 November 2016 in Ny-Ålesund: **a)** Radiosonde profile between 10:48 -11:24 UTC (0 and 10 km height). Relative humidity (RH) with respect to water in blue and relative humidity with respect to ice in red. **b)** Radar reflectivity factor Z . The red vertical line visualises the ascend of the radiosonde. The black vertical lines visualise the time period considered for analysing the radar data. The red horizontal lines and the numbers 1,2,3 and 4 visualise the subsaturated layers. The grey colour visualises the subsaturated layers. At the time when the radiosonde reached the supersaturated layer 1 at 3.85 km ~~due to horizontal wind drift~~ the radiosonde is 3.683,70 km away from the radar due to horizontal wind drift.

Ny-Ålesund ~~-The (hereafter called the radar data). Out of the~~ continuous radar data ~~has to be averaged. Here we choose~~ the start time ~~is chosen to be~~ 30 minutes before the radiosonde launch and the end time ~~is to be~~ 30 minutes after the radiosonde reached 10 km height. Additionally we calculate the average time due to wind advection of the radiosonde away from the radar. We delay the start and end time of the included radar data by this. For the 3 November 2016 the evaluated time period of the

5 radar data is visualised by black lines in Fig. 3b. The heights of the super- and subsaturated layers, derived from the radiosonde humidity measurement, are indicated by red horizontal lines in Fig. 3b. In the *supersaturated layer above* only the lowest part is of interest for potential ice crystal seeding, since from here the ice crystal might fall. We consider only the lowermost 100 m of this ~~supersaturated layer. A measured radar reflectivity factor above the detection limit means that cloud droplets or ice crystals reflect the radar signal back. No radar reflectivity factor data means that the detection limit of -67 at 100~~supersaturated layer

10 above (see Fig. to -38 at 10 was not reached (Küchler et al., 2017). The averaged radar data is evaluated regarding if 2). If more than 50 % of the ~~datapoints selected radar data~~ selected radar data contain radar reflectivity factor data (coloured in Fig. 3b) ~~meaning that cloud droplets or ice crystals were present. If so, then~~ it is defined as cloud by the algorithm. If less than 50 % ~~of the data~~

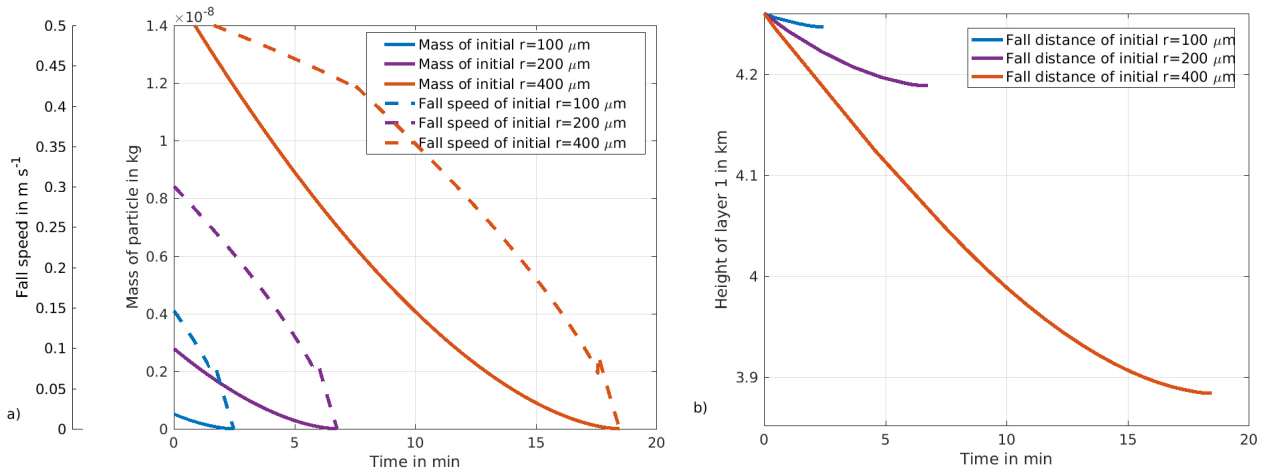


Figure 4. Calculation of sublimation for the layer 1 between 4.26 km and 3.85 km height at 3 November 2016: **a)** Fall speed and change of mass of ice crystal with time. **b)** Fall distance of ice crystal with time. The evaluated initial ice crystal sizes are $r = 50$ 100 μm , 100 200 μm and 150 400 μm .

~~points~~ contain radar reflectivity factor data (white in Fig. 3b), then it is defined as ~~no-cloud~~ .not cloud containing. For the *subsaturated layer in between* only the ~~lowest part is evaluated~~ lowermost 100 m are analysed in order to address the question if the ice crystal survives so far. ~~The lowermost 100 are considered, but if~~ If the layer is thinner than 100 m only the available vertical thickness is considered. Again, if more than 50 % contain radar reflectivity factor data, it is considered as cloud. If less than 50 % contain radar reflectivity factor data, it is considered as no cloud. In the *supersaturated layer below* any radar signal at any height is of interest for potential ice crystal seeding. As soon as the ice crystal reaches this supersaturated layer it has survived. The ice crystal ~~does not decrease in size, so that it~~ begins to grow and can influence a cloud no matter at which height it is within the supersaturated layer. For the *supersaturated layer below* the algorithm, starting from the top, searches for any layer of 100 m containing more than 50 % radar reflectivity factor data. If no layer of 100 m containing more than 50 % radar reflectivity factor data is found, at the lower boundary of this supersaturated layer the evaluated vertical thickness is decreased until 20 m. If no layer contains more than 50 % radar reflectivity factor data, it is considered that no cloud is present in this layer (*no cloud*). In the example of 3 November 2016 (Fig. 3) the *supersaturated layer above* the *subsaturated layer 1* is cloud containing (*cloud above*), the *subsaturated layer 1* is not cloud containing (*no cloud in between*) and the *supersaturated layer below* is cloud containing (*cloud below*). The classification sorts the 3 November 2016 as MLC case. Analysing each combination of *supersaturated layer above*, *subsaturated layer in between* and *supersaturated layer below* results in the eight different cloud categories presented in Table 1.

~~For the non-seeding cases the classification considers~~ The classification sorts the cloud category 8 (*cloud above, no cloud in between, cloud below* ) as MLC for the non-seeding cases (purple and red in Fig. 1). We here refer to the MLC def-

Table 1. Overview of the classification into eight different cloud categories. N means no cloud and C means cloud. SLC means single-layer cloud, MLC means multilayer cloud.

	Cloud category #							
	1	2	3	4	5	6	7	8
								
above	N	N	N	N	C	C	C	C
in between	N	N	C	C	C	C	N	N
below	N	C	C	N	C	N	N	C
	no cloud	SLC	SLC	SLC	seeding MLC	SLC	SLC	non-seeding MLC

initiation of two separate clouds with clear visible interstice in between (Liu et al., 2012). ~~Since seeding ice crystals result in a signal in the radar data, it is difficult to distinguish this radar signal from the radar signal caused by cloud particles (Verlinde et al., 2007, 2013). The classification includes therefore for~~ Additionally, for including the seeding cases, the cloud category 5 (cloud above, cloud in between, cloud below ) is sorted as MLC (light green and yellow in Fig. 1). ~~Indeed, since seeding ice crystals result in a signal in the radar data, it is difficult to distinguish this radar signal from the radar signal caused by cloud particles (Verlinde et al., 2007, 2013).~~ Therefore the classification's result should be treated as upper limit for MLC occurrence. A multilayer cloud containing several subsaturated layers of which some can be seeding and some non-seeding (at least one of each kind) is sorted as own multilayer category (orange in Fig. 1). The 3 November 2016 is an example to this category since layer 1 is a non-seeding layer and the layers 2, 3 and 4 are seeding layers. The classification sorts the cloud category 1 (no cloud above, no cloud in between, no cloud below ) as no cloud (light blue in Fig. 1). The cloud categories 2 () , 3 () , 4 () , 6 () , 7 () are sorted as single-layer cloud (turquoise in Fig. 1). In the following section we show the results given by our classification for the one-year dataset used for the analysis.

3 Results and discussion of the classification applied to the Ny-Ålesund dataset

3.1 Results of classification step 1

The classification step 1 evaluates relative humidity profiles in order to detect seeding and non-seeding subsaturated layers. For the sublimation calculation primarily ~~an a hexagonal plate with~~ initial ice crystal size of $r = 100$ ~~400~~ μm is used. The result is presented in Fig. 5. The criteria for potential MLC detection in classification step 1 is the combination of a *supersaturated layer above*, a *subsaturated layer in between* and a *supersaturated layer below*. This combination occurs in 6869% of the profiles (2223% yellow + 2829% orange + 1817% red in Fig. 5), which means that in 6869% of the analysed radiosonde profiles we find potential MLCs. The possibility of microphysical interaction by seeding exists in 5052% . ~~Varying the initial ice crystal size has a large, non-linear~~ A seasonal cycle (Fig. 6) in this one-year dataset is not visible. In several months the amount of non-seeding layers is larger or similar to the amount of seeding layers. However, we only analysed a time period

of one year, a seasonal cycle might become more distinct when analysing a longer time period. The impact of the ice crystal shape is shown in Fig. A1. In comparison to the hexagonal plate as a standard, the rimed columns result in more seeding cases and the sectored plates result in less seeding cases. This is in agreement with Mitchell (1996), saying rimed particles falling faster than non-rimed particles. The aggregates show the most seeding cases and this matches the large fall speed provided by Mitchell (1996). In contrast to the ice crystal shape, the ice crystal size has a larger impact on the distribution between seeding and non-seeding subsaturated layers. A smaller initial ice crystal size leads to more non-seeding layers and a larger initial ice crystal size leads to more seeding layers (numbers in brackets in Fig. 5). A seasonal cycle (Fig. 6) in this one-year dataset is not visible. The possibility of seeding changes from 39 % for the ice crystal size $r = 100 \mu\text{m}$ to 46 % for the ice crystal size $r = 200 \mu\text{m}$ and to 52 % for the ice crystal size $r = 400 \mu\text{m}$. The impact is non-linear and indicates that towards smaller ice crystals the impact of ice crystal size on the possibility of seeding becomes more important.

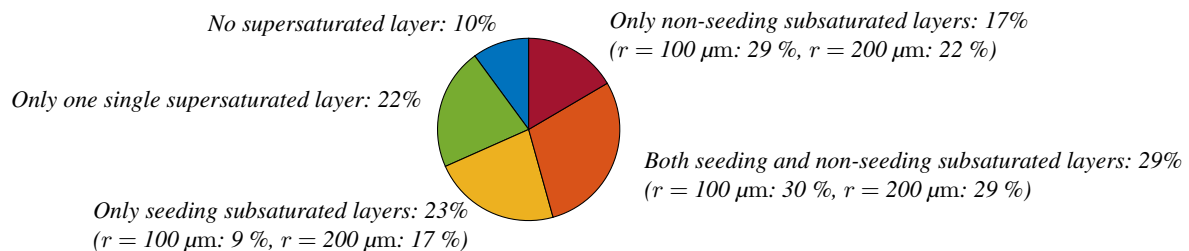


Figure 5. Classification step 1 using an a hexagonal plate as initial ice crystal with the size of $r = 400 \mu\text{m}$: Relative occurrence of supersaturated layers and seeding and non-seeding subsaturated layers. 100 % equals 278 relative humidity profiles. Percentages in brackets refer to the calculation using the initial ice crystal sizes $r = 100 \mu\text{m}$ and $200 \mu\text{m}$. For the categories 'no supersaturated layer' and 'only one single supersaturated layer' there are no changes in percentage. The values are rounded to zero decimal places.

3.2 Results of classification step 2

In many cases of the 68 Relative humidity data alone is not sufficient to detect MLC cloud occurrence and hence radar data is included in the classification step 2. The 69 % potential MLC occurrence the results obtained by the radiosonde profiles disagree with actual MLC occurrence observed by the radar. In order to cross-check actual gained in classification step 1 are now cross-checked for actual cloud occurrence in the supersaturated layer above, in the subsaturated layer in between and in the supersaturated layer below; radar data is included in the classification step 2. Including. Including the radar data leads to eight different cloud categories (Sect. 2.3). These cloud categories are then separated regarding if the subsaturated layer in between is a non-seeding or seeding case according to step 1. For the non-seeding cases the cloud categories are shown in Fig. 7. The cloud category 8 (cloud below, no cloud in between, cloud above) is counted as MLC and therefore coloured purple. All other cloud categories occurring (1,2,3,5,7) are not considered as MLCs and are therefore coloured dark grey and light grey. There is a high amount of the cloud category 1 (For the seeding cases the cloud categories are shown in Fig. 8. The cloud

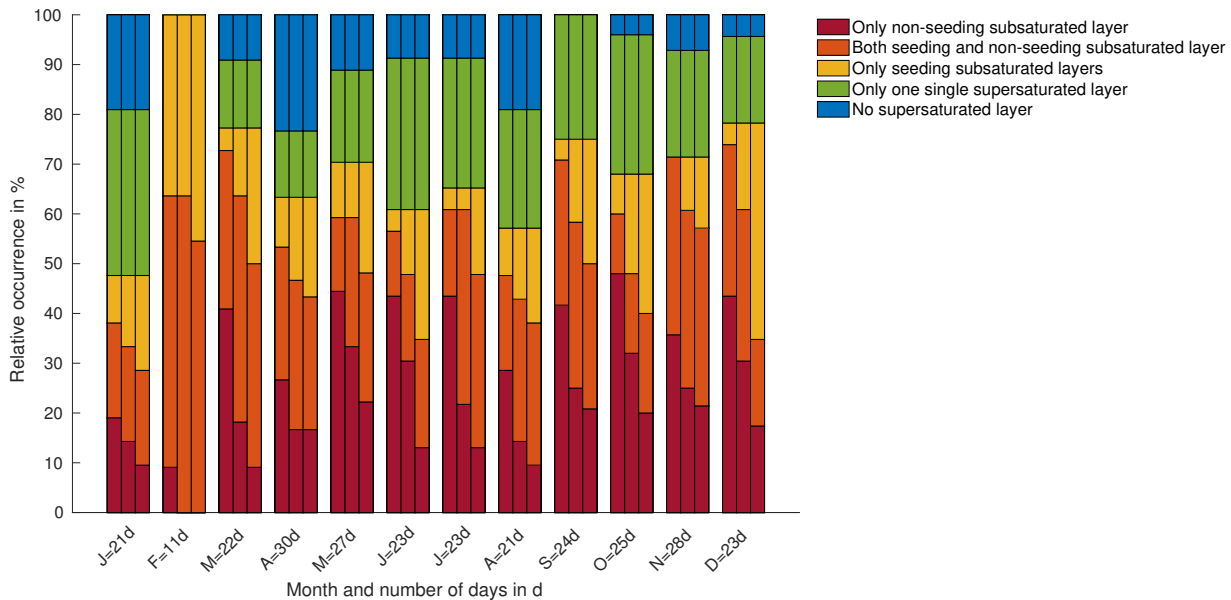


Figure 6. Temporal distribution of MLC days using classification step 1. For each month the left bar refers to the initial ice crystal size $r = 50100$ μm , the middle bar refers to the initial ice crystal size $r = 100200$ μm and the right bar refers to the initial ice crystal size $r = 150400$ μm . On the x-axis the given number in the labels refers to the number of days (d) considered for the specific month.

category 8 (no cloud below, no cloud in between, no cloud above, dark grey in Fig. 7) does hardly occur. This is explained by the fact that seeding ice crystals will make a signal in the radar reflectivity data. Therefore the cloud category 5 (cloud above, cloud in between, cloud below) is considered as seeding MLC and coloured light green in Fig. This means no cloud is visible in the radar even though a potential MLC was detected in the radiosonde profiles. Even if the 8. For distinguishing a seeding MLC from a single-layer cloud a lidar/ceilometer detecting multiple cloud layers would be needed. In both the non-seeding and seeding case there is a high amount of ice-supersaturated layers above and below are supersaturated with respect to ice, the lack of suitable IN can prevent cloud formation (dark grey in Fig. missing cloud formation. 7 and Fig. 8). Therefore including radar data is of importance to the MLC classification. Ice supersaturation without cloud formation is a global phenomena in the upper troposphere and does also occur in the Arctic (Spichtinger et al., 2003). Spichtinger et al. (2002) explains this ice-supersaturation without cloud formation with the lack of aerosol as IN. Also for the cloud categories These cloud categories are 1 (no cloud below, no cloud in between, no cloud above), 2 (no cloud above, no cloud in between, cloud below), 6 (cloud above, dark grey in Fig. 7 cloud in between, no cloud below) and 7 (cloud above, no cloud in between, no cloud below, -), all dark grey in Fig. 7) too little IN can explain the and Fig. 8. In the ice-supersaturated layers above and below missing cloud formation in the supersaturated layers. For cloud category 2 in the seeding case can be explained by the lack of aerosol as INP (Spichtinger et al., 2002). Ice-supersaturation without cloud formation is a global phenomena in the upper troposphere and does also occur in the Arctic (Spichtinger et al., 2003). In the seeding case of cloud category 2 additionally the formation of

seeding ice crystals is prevented (~~dark grey in Fig. 8~~). ~~Besides the possible lack of IN also~~. Indeed, a very low liquid and ice water content could also result in a value below the radar sensitivity limit explaining these cases. Other contradictions between relative humidity and radar data can be explained by the horizontal drift of the radiosonde away from the radar and inaccuracies due to time averaging of the radar data ~~can explain contradictions between radiosonde profiles and radar~~ (light grey in Fig. 5 and Fig. 6). ~~This leads to the~~ The cloud signal inside the subsaturated layer in the cloud categories 3 (*no cloud above, cloud in between, cloud below*; ~~light grey in Fig. 7~~) and ~~) and in the seeding case 5~~ (*cloud above, cloud in between, cloud below*; ~~light grey in Fig. 7~~) where a cloud signal is measured inside the subsaturated layer and ~~) can be explained by this and therefore~~ these cloud categories are ~~not counted~~ rejected as MLCs. Additionally, the minimum detection height of 223 m might lead to some cases not being considered.

10 ~~For the seeding subsaturated layers the cloud categories are shown in Fig. 8. The cloud category 8 (cloud below, no cloud in between, cloud above) does not occur. This is explained by the fact that seeding ice crystals will make a signal in the radar reflectivity data. The cloud category 6 (cloud above, cloud in between, no cloud below) is a seeding case, but since the lower cloud layer is missing, no MLC case. The cloud categories 1,2,7, where missing cloud activation can be explained by missing IN, are coloured dark grey. The cloud category 5 (cloud above, cloud in between, cloud below) is coloured light green in Fig. 8 and is considered as seeding MLC. For distinguishing a seeding MLC from a single layer cloud a lidar/ceilometer detecting multiple cloud layers would be needed.~~

In Fig. 9 the result of the cloud classification step 2 using both radiosonde profiles and radar is presented. MLCs occur in 29 % of the investigated profiles (6 % 'only non-seeding', red + 3 % 'both seeding and non-seeding', orange + 20 % 'only seeding' MLC, yellow). Single-layer clouds occur in 50 % of the investigated profiles (28 % 'multilayer cloud by radiosounding, but single-layer cloud by radar', turquoise + 22 % 'single-layer clouds by radiosounding', green). No cloud layer occurs in 22 % of the investigated profiles (12 % 'multilayer cloud by radiosounding, but not cloud by radar', light blue + 10 % 'no cloud by radiosounding', dark blue). A seasonal variation (Fig. 10) in between months in this one-year dataset is very weak for the MLC categories ('only non-seeding multilayer clouds', 'both seeding and non-seeding multilayer clouds' and 'only seeding multilayer clouds'). There is a slight increase in MLC occurrence between July and November and February to March.

25 The impact of different ice crystal sizes used in classification step 2 is presented as numbers in brackets in Fig. 9 and as bars in Fig. 10. The main impact is that for a smaller ice crystal there are less 'only seeding multilayer cloud' cases and more 'multilayer cloud by radiosounding, but single-layer cloud by radar' cases. This is explained by the cloud category 5 ('*cloud above, cloud in between, cloud below*') occurring frequently and sorted as MLC in the seeding cases and as single-layer cloud in the non-seeding cases. Because of this different sorting of seeding and non-seeding cases, the impact of the ice crystal size is less strong in classification step 2 compared to step 1. The impact of the different ice crystal shapes is even less, almost not visible.

A sensitivity how the results would change assuming an uncertainty of the radiosonde humidity of $\pm 5\%$ is shown in Appendix Fig. A2 and Fig. A3. The measurement uncertainties lead to variations in the results of the same order of magnitude as when varying the ice crystal size. If the relative humidity is on average overestimated, the impact on the results is of smaller importance than if the relative humidity is on average underestimated. This might be explained by the minimum thickness

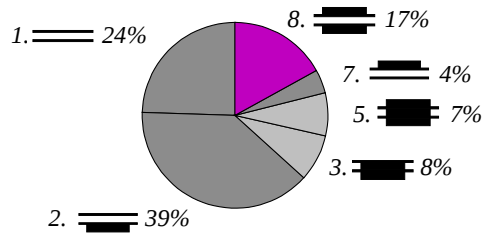


Figure 7. Non-seeding cases: Cloud categories of all non-seeding subsaturated layers. *In between* refers to the subsaturated layer. *Above* and *below* refers to the supersaturated layers above or below the subsaturated layer. 100 % equals all non-seeding subsaturated layers. Non-seeding is calculated using ~~an ice crystal~~ a hexagonal plate of the initial size $r = 100400$ μm . The values are rounded to zero decimal places.

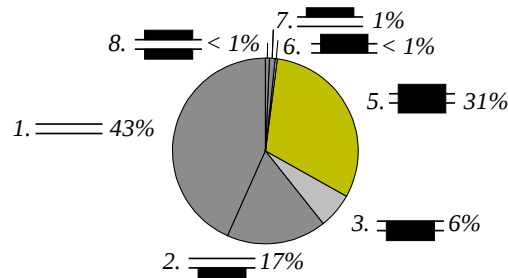


Figure 8. Seeding cases: Cloud categories of all seeding subsaturated layers. *In between* refers to the subsaturated layer. *Above* and *below* refers to the supersaturated layers above or below the subsaturated layer. 100 % equals all seeding subsaturated layers. Seeding is calculated using ~~an ice crystal~~ a hexagonal plate of the initial size $r = 100400$ μm . The values are rounded to zero decimal places.

threshold of 100 m used for identifying supersaturated and subsaturated layers limiting the effect when overestimating the relative humidity.

3.3 Discussion and evaluation of the results using skill scores

For evaluating the MLC occurrence derived by the classification steps 1 and 2 skill scores are used. First classification step 1 (using only radiosonde data) is compared to classification step 2 (using both radiosonde and radar). Secondly classification step 2 is compared to a visual inspection. The visual inspection is done manually. We inspect the radar images and decide whether it is a visual MLC or no visual MLC. For the visual inspection we consider a shorter time ~~periode~~ period like that of the radiosonde ascent rather than the average over one hour like the detection algorithm does. ~~Small cloud stains are~~ A

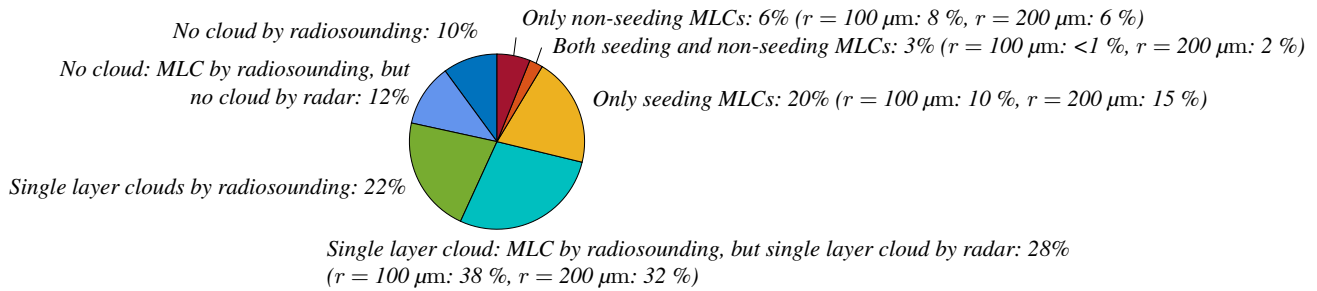


Figure 9. Cloud occurrence derived from using both radiosonde and radar for detection. For the categories the same colours as in Fig. 1 are used. 100 % equals 278 days (analysed days within the one-year data set). Seeding and non-seeding is calculated using an ice crystal a hexagonal plate of the initial size $r = 100/200 \mu\text{m}$. Percentages in brackets refer to the calculations using different initial ice crystal sizes $r = 50/100 \mu\text{m}$ and $150/200 \mu\text{m}$. The values are rounded to zero decimal places.

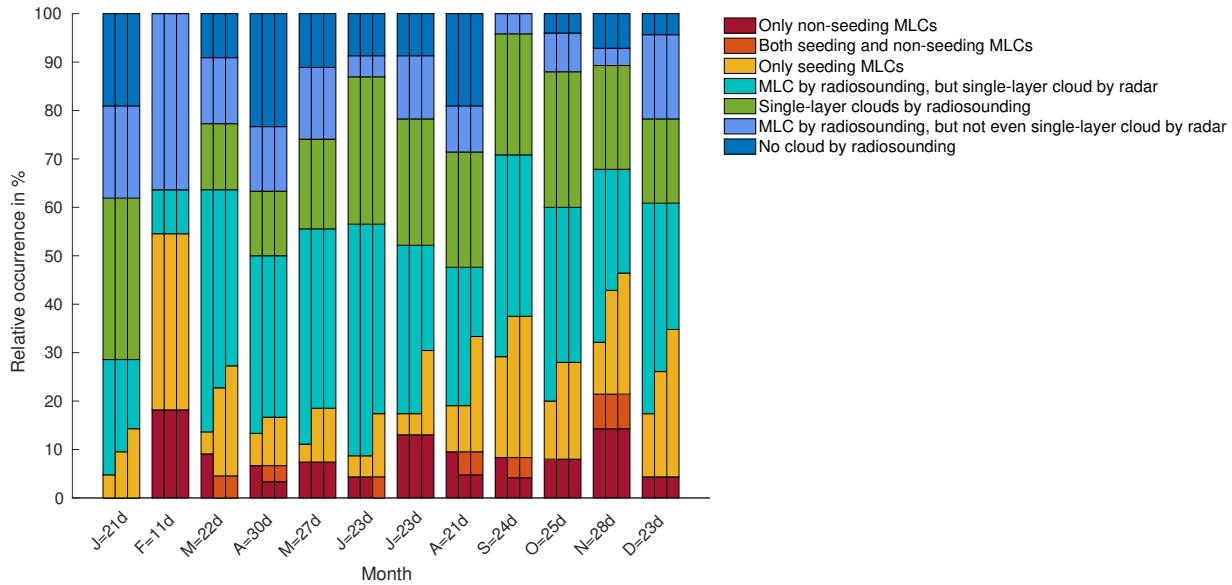


Figure 10. Temporal distribution of MLC days using classification step 2. For each month the left bar refers to the initial ice crystal size $r = 50/100 \mu\text{m}$, the middle bar refers to the initial ice crystal size $r = 100/200 \mu\text{m}$ and the right bar refers to the initial ice crystal size $r = 150/400 \mu\text{m}$. On the x-axis the given number in the labels refers to the number of days (d) considered for the specific month.

longer radar signal only existing of small strains is not counted as clouds and clouds containing cloud and a longer radar signal containing some small cloud free holes are counted as clouds is counted as cloud.

The variables A, B, C, D needed for deriving the skill scores are given as in Table 2. Out of these variables the probability of detection POD is defined as

$$POD = \frac{A}{A+C} \quad (8)$$

and shows perfect detection at $POD = 1$ and no detection at $POD = 0$.

The false alarm rate FAR is defined as

$$5 \quad FAR = \frac{B}{A+B} \quad (9)$$

and gives $FAR = 0$ for no false alarms and $FAR = 1$ for only false alarms.

The Heidke skill score HSS

$$HSS = 2 \frac{AD - BC}{(A+C)(C+D) + (A+B)(B+D)} \quad (10)$$

evaluates the total predictability with values reaching from $HSS = -\infty$ to 1. $HSS = 0$ means that there is no predictability.

Table 2. Skill score evaluation: Definitions of the evaluation variables A, B, C, D used for the evaluation of the MLC occurrence derived by the classification steps 1 and 2 in comparison to a best estimate of MLC occurrence.

		Best estimate	
		MLC	no MLC
Classification	MLC	A	B
	no MLC	C	D

For the evaluation of classification step 1 (using only radiosonde) the variables A, B, C, D are presented in Table 3. There
10 the results of classification step 1 are divided into MLC and no MLC. MLCs in classification step 1 are defined as one *su-
persaturated layer above*, one *subsaturated layer in between* and one *supersaturated layer below*. If a MLC is detected by
classification step 1, the best estimate for evaluation is given by classification step 2 (MLC or no MLC by radar). If no MLC
is detected by classification step 1, the best estimate for evaluation is done by the manual visual inspection of the radar im-
ages. The manual visual inspection is necessary owing to the non-existence of classification step 2 if there is no MLC by
15 radiosounding. Out of Tab. 3 we see that classification step 1 represents a reliable upper limit (28.8 % + 39.6 % = 68.4 %) for identifying MLC days, but the actual number might be as low as less than the half (28.8 %). In Table 4 the resulting skill
scores are shown. The limited predictability leads to a low Heidke skill score of $HSS = 0.31$ for $r = 400 \mu\text{m}$. The good POD
of 0.99 (for $r = 400 \mu\text{m}$) affirms that there is no big loss of MLC cases when applying classification step 1 (only 0.4 % for
 $r = 400 \mu\text{m}$). Varying the initial ice crystal size to $r = 50$ and $r = 150$ does almost not cause any variation of POD . This
20 means the impact of chosen initial ice crystal size on the predictability is limited. FAR being 0.58 reveals that about half of
the MLC estimated from radiosonde humidity measurements is 'no MLC by radar'. Therefore classification step 1 represents a reliable upper limit (68.4 %) for identifying MLC days, but the actual number might be as low as less than the half (28.8 %).

~~This limited predictability leads to a low Heidke skill score of $HSS = 0.31$ for~~ It becomes clear that the use of the radiosonde data on its own does not reliably identify the occurrence of MLCs, but can be used in combination with radar data to give information on the presence of MLCs. Reducing the initial ice crystal size to $r = 100 \mu\text{m}$ or $r = 200 \mu\text{m}$ shows a reduced Heidke skill score. This indicates that the chosen initial ice crystal size impacts the predictability.

Table 3. Evaluation of the MLC results of radiosonde detection (classification step 1) in comparison to radar detection (classification step 2). 'MLC by radar' is given by cloud category 8 for the non-seeding cases and by cloud category 5 for the seeding cases. The evaluation is done for the ice crystal sizes $r = 50$ 100 μm , ~~100~~200 μm and ~~150~~400 μm . The values are rounded to one decimal place.

	$r = 100 \mu\text{m}$		$r = 200 \mu\text{m}$		$r = 400 \mu\text{m}$	
	MLC by radar	no MLC by radar	MLC by radar	no MLC by radar	MLC by radar	no MLC by radar
MLC by radiosounding	19.8 <u>18.7</u> %	48.6 <u>49.6</u> %	28.8 <u>24.1</u> %	39.6 <u>44.2</u> %	29.1 <u>28.8</u> %	39.2 <u>39.6</u> %
no MLC by radiosounding	0.4 %	31.3 %	0.4 %	31.3 %	0.4 %	31.3 %

Table 4. Skill scores for comparison of MLC results of radiosounding and radar. The skill scores are calculated for the ice crystal sizes $r = 50$ 100 μm , ~~100~~200 μm and ~~150~~400 μm . The values are rounded to two decimal places.

	$r = 50$ <u>100</u> μm	$r = 100$ <u>200</u> μm	$r = 150$ <u>400</u> μm
<i>POD</i>	0.98	0.99	0.99
<i>FAR</i>	0.71 <u>0.73</u>	0.58 <u>0.65</u>	0.57 <u>0.58</u>
<i>HSS</i>	0.20 <u>0.19</u>	0.31 <u>0.25</u>	0.31

5 Next we evaluate classification step 2 and the results are presented in Table 5 and Table 6. Due to the missing possibility to distinguish falling ice crystals from cloud particles in the radar image, including seeding to our classification leads to high uncertainties. Therefore for evaluating classification step 2, we only consider the non-seeding MLCs (cloud cat. 8). This is a similar approach as done by Intrieri et al. (2002), who defined MLCs as two separate clouds with clear visible interstice in between. For the evaluation of classification step 2 we use the manual visual inspection as best estimate. Also for the manual
10 visual inspection we do not account for the possibility of seeding, meaning that we count a connected radar signal in the vertical as single-layer cloud.

Classification step 2 classifies ~~8.37~~9 % MLCs ($r = 100$ 400 μm in Tab. 5). This represents a lower limit for identifying MLC days, since classification step 2 is not able to classify ~~10.1~~10.4 % (4.0 % are classified as seeding MLC and 6.1 % as no MLC). The actual number of MLCs might therefore be twice as high (~~8.37~~9 % + ~~10.1~~10.4 % = ~~18.4~~18.3 % for $r = 100$ 400 μm).
15 This limited probability is underlined by *POD* being ~~0.45~~0.43 (Tab. 6). Problems of the classification are given by the not exact accordance between radiosonde profile and radar. While the radiosonde ascents, it is horizontally drifted away from the radar by wind. Additionally the radar measurements have to be averaged over time and this is not done by the visual inspection. An existing cloud, which is too weak or too short lasting in the radar image, can therefore lead to discrepancies between the classification and the visual detection. A too high cloud top or base compared to the relative humidity threshold,

a missing relative humidity layer or too many relative humidity layers in a not changing radar image do also cause erroneous classification.

However, few false alarms (~~0.40.7~~ % for $r = 100$ ~~400~~ μm) cause a low FAR of ~~0.04~~~~0.08~~. This reveals predictability by a HSS skill score of ~~0.56~~. ~~A larger radius ($r = 150$) leads to more seeding cases. This results in less non-seeding MLCs accounted for in classification step 2 and worsens therefore the predictability for $r = 150$ ($HSS = 0.47$) in comparison to $r = 100$ ($HSS = 0.56$).~~ ~~0.53~~. Using the smaller radius of $r = 50$ ~~200~~ μm does not change the results. Even if there is less seeding, these cases belong to the category 'both seeding and non-seeding' and do therefore not change the results. Using the even smaller radius of $r = 100$ μm does impact the results. In classification step 1 the larger radii $r = 100$ ~~200~~ μm and $r = 150$ ~~400~~ μm lead to the best Heidke skill score ($HSS = 0.25$ and 0.31) in comparison to the small radius. However, in classification step 2 the smaller radii ~~radius~~ $r = 50$ and $r = 100$ μm lead to the best Heidke skill score ($HSS = 0.56$) ~~in comparison to 0.55~~. ~~Even if the large radius of $r = 150$ ~~400~~ μm . In this way we decided to focus on the radius is likely in mixed-phase MLCs (Mioche et al., 2016), it is possible that it does not occur as often as a radius of $r = 100$ μm in the previous sections of this manuscript.~~

Table 5. Evaluation of the MLC results including only the non-seeding MLC of the classification step 2 in comparison to manual visual detection. 'Non-seeding MLC' includes 'only non-seeding' and 'both seeding and non-seeding' MLC. 'Seeding MLC and no MLC' includes seeding MLCs, single-layer clouds and no cloud layers. The evaluation is done for the ice crystal sizes $r = 50$ ~~100~~ μm , ~~100~~~~200~~ μm and ~~150~~~~400~~ μm . The values are rounded to one decimal place.

	$r = 100 \mu\text{m}$		$r = 200 \mu\text{m}$		$r = 400 \mu\text{m}$	
	visual MLC	no visual MLC	visual MLC	no visual MLC	visual MLC	no visual MLC
non-seeding MLC	8.3 %	0.40.7 %	8.37.9 %	0.40.7 %	6.57.9 %	0.00.7 %
seeding MLC and no MLC	10.1 %	81.380.9 %	10.110.4 %	81.380.9 %	11.910.4 %	81.780.9 %

Table 6. Skill scores for comparison of MLC results of the non-seeding cases of the classification step 2 and the visual detection. The skill scores are calculated for the ice crystal sizes $r = 50$ ~~100~~ μm , ~~100~~~~200~~ μm and ~~150~~~~400~~ μm . The values are rounded to two decimal places.

	$r = 100 \mu\text{m}$	$r = 200 \mu\text{m}$	$r = 400 \mu\text{m}$
POD	0.45	0.45 0.43	0.35 0.43
FAR	0.04 0.08	0.04 0.08	0.00 0.08
HSS	0.56 0.55	0.56 0.53	0.47 0.53

4 Conclusions

15 In this work we use in-situ profiling by radiosondes and ground-based remote sensing by vertically-pointing cloud Doppler radar to identify Arctic MLCs between 0 - 10 km height. We evaluate relative humidity profiles regarding an ice-subsaturated

layer in between two ice-supersaturated layers. This combination occurs in 68.4 % out of 278 analysed days (only one hour each day is analysed) using the minimum considered thickness for the supersaturated and subsaturated layers of 100 m. A high amount of supersaturated layers found in the radiosonde profiles does not coincide with observed cloud occurrence, probably due to lack of CCN and INP and thereby missing cloud activation. Only using radiosonde profiles is not sufficient
5 for the detection of clouds. Therefore the classification is expanded by using radar data for excluding non relevant cases. The extended classification leads to 29 % MLCs with a very weak seasonal cycle. We investigate these MLC further regarding the possibility of seeding, which means if an ice crystal of the size $r = 100400 \mu\text{m}$ ~~can survive sublimation~~ does not fully sublimate in the subsaturated layer when falling through this layer. We find that seeding can potentially occur in 23 % of the 278 investigated days. In these cases there is a radar signal in the subsaturated layer in between the two cloud layers. Here it
10 remains as an unsolved question if this is actually due to seeding (falling ice crystals in between the two cloud layers) or due to one continuous cloud layer. Since the percentage for potentially seeding is as high as 23 %, the importance of seeding on the lower cloud is not negligible. The effects of the seeding on the lower cloud could be an increase in cloud ice, and thereby precipitation formation and cloud dissipation. In order to gain more information about the existence of these ice crystals, further measurements of e.g. lidar would be needed.

15 Non-seeding means that the subsaturated layer is too thick or too dry for the ice crystal to survive the sublimation. Non-seeding MLCs are visible in the radar as two separated cloud layers and this occurs in 9 % of the analysed days. ~~While it could have been envisioned that falling ice crystals occur in low concentrations below the radar detection limit.~~ Following from our sublimation calculation we find that MLCs visible separated in the radar are unable to interact through seeding ~~following from our sublimation calculation~~. However, we have to keep uncertainties like the radar detection limit in mind. In the case of
20 non-seeding MLCs, radiative interactions, like a weakening of the lower cloud in the existence of a higher cloud, can occur. These interactions are most likely not captured correctly by weather models. However, the 9 % occurrence implies that clearly separated MLCs should probably not be neglected in weather models.

Cloud detection by satellites is challenging in the Arctic, but Liu et al. (2012) found Arctic MLCs to occur between 17 - 25 % of the investigated time. However, since the minimum considered cloud thickness was as big as 960 m, they assumed
25 their MLC amount most likely to be underestimated. In order to evaluate our classification we compare our results to a manual visual inspection of the radar observations. Since the seeding cases can not be separated from single-layer cloud cases and therefore cause uncertainties, the seeding cases are excluded in the evaluation. The evaluation results in non-seeding MLC occurrence of 9 % being a reliable lower limit. However, the Heidke skill score HSS for prediction is only ~~0.560.53~~. Changing the ice crystal size has ~~only little various impacts. For smaller ice crystal sizes the~~ impact on the results ~~Neither a smaller~~
30 ~~initial ice crystal size of $r = 50$ nor a larger initial is larger. However, the skill score analysis showed no clear answer about the best choice of~~ ice crystal size ~~of $r = 150$ leads to major improvements.~~ Erroneous detection is often caused by super- and subsaturated layers identified in the radiosonde data not overlapping with the radar cloud top and base. Also non-relevant, often thin super- and subsaturated layers cause problems. Here the uncertainties in the relative humidity measurements and the chosen minimum height limits have to be kept in mind when examining these disagreements. The manual visible inspection
35 results in 18.4 % non-seeding MLC occurrence.

Using our ground-based classification leads to a MLC occurrence between 8 - 29 % for Ny-Ålesund. If and how much this number will differ at a more typical high Arctic location, with less cyclonic and orographic influence but rather stable conditions caused by sea ice, remains an unsolved question. We show that seeding is more frequently possible than non-seeding and always causes a signal in the radar. Therefore uncertainties remain when distinguishing MLC from single-layer clouds in radar images. While extensive modelling studies (e.g. Klein et al. (2009) and Ovchinnikov et al. (2014)) have dealt with single-layer Arctic clouds, we suggest that the more complex microphysics and radiative properties of MLCs and their changes due to aerosol and climate ~~pertubations~~perturbations should be a focus of future research.

Code and data availability. The code for the seeding/non-seeding multilayer cloud detection algorithm was written in Matlab and is available at https://github.com/maikenv/Classification_algorithm_of_multilayer_clouds.git. The radiosonde data is available through Sommer et al. (2012) and Maturilli (2017). The radar data is part of the (AC)³ project and was provided by Kerstin Ebell.

Appendix A

Table A1. Calculation of capacitance based on Westbrook et al. (2008). The listed ice crystal shapes correspond to the selected particles hexagonal plates, rimed long columns, crystal with sector-like branches, and assemblages of planar polycrystals respectively (Mitchell, 1996). $2a$ refers to the maximum span across the basal/hexagonal face (Westbrook et al., 2008). In the case of the hexagonal plate and the star crystal this is $a = r$. In the case of a hexagonal column it is $a = 2r/A$, with $2r$ being the maximum dimension.

	Aspect ratio A	Capacitance C	Capacitance C in m for $r = 400 \mu\text{m}$
Hexagonal plate	0.05	$C = 0.58(1 + 0.95 \cdot A^{0.75})a$	$\approx 2.55 \times 10^{-4}$
Hexagonal column	5	$C = 0.58(1 + 0.95 \cdot A^{0.75})a$	$\approx 3.88 \times 10^{-4}$
Star crystal	0.3	$C = 0.596(1 - 0.38e^{-4.7A})a$	$\approx 2.16 \times 10^{-4}$
Aggregates	-	$C = 0.25 \cdot 2 \cdot r$	$\approx 2.00 \times 10^{-4}$

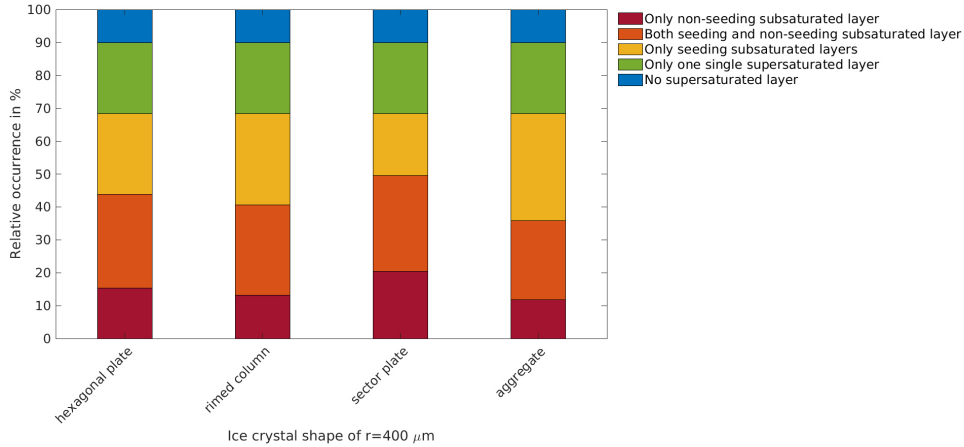


Figure A1. Cloud occurrence derived by using classification step 2 using the four different ice crystal shapes: hexagonal plate, rimed column, sector plate, aggregate. The initial ice crystal size is $r = 400 \mu\text{m}$.

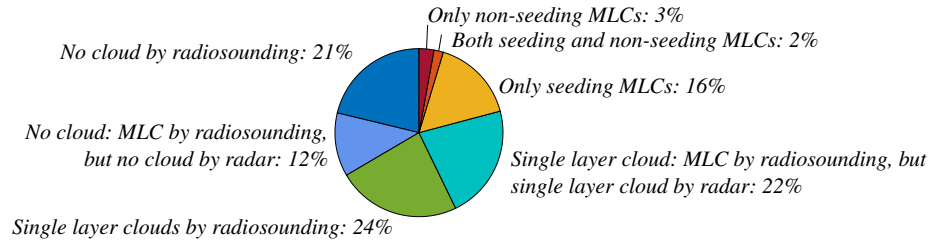


Figure A2. Cloud occurrence derived from using both radiosonde and radar for detection. For the radiosonde data the measurement uncertainty is considered to be -5 % over the whole radiosonde profile. Seeding and non-seeding is calculated using an ice crystal of the size $r = 100\text{400}\ \mu\text{m}$. The values are rounded to zero decimal places.

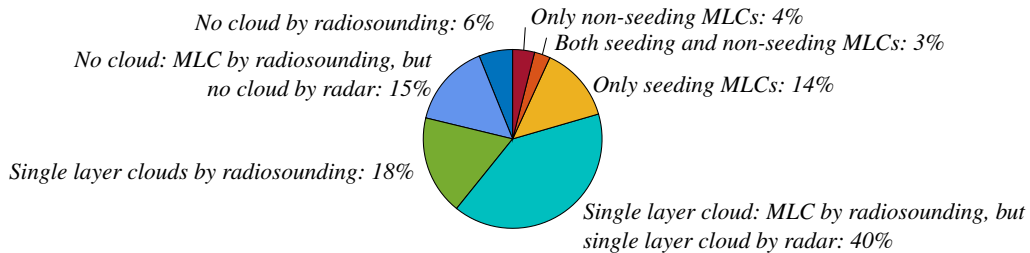


Figure A3. Cloud occurrence derived from using both radiosonde and radar for detection. For the radiosonde data the measurement uncertainty is considered to be +5 % over the whole radiosonde profile. Seeding and non-seeding is calculated using an ice crystal of the size $r = 100\text{400}\ \mu\text{m}$. The values are rounded to zero decimal places.

Competing interests. The authors confirm that they have no conflict of interest.

Acknowledgements. We gratefully acknowledge support by the SFB/TR 172 “Arctic Amplification: Climate Relevant Atmospheric and Surface Processes, and Feedback Mechanisms (AC)³ funded by the DFG (Deutsche Forschungsgesellschaft). In particular, the cloud radar observations are performed within the sub-project E02 of SFB/TR 172 and have been provided by Kerstin Ebell. The radiosonde data was
5 provided by the Alfred Wegener Institute. Luisa Ickes acknowledges the Swiss National Science Foundation (Early Postdoc.Mobility) for support.

References

- Andronache, C., ed.: *Mixed-Phase Clouds*, Elsevier, 2018.
- Avramov, A. and Harrington, J. Y.: Influence of parameterized ice habit on simulated mixed phase Arctic clouds, *Journal of Geophysical Research: Atmospheres*, 115, 2010.
- 5 Barrett, A. I., Hogan, R. J., and Forbes, R. M.: Why are mixed-phase altocumulus clouds poorly predicted by large-scale models? Part 1. Physical processes, *Journal of Geophysical Research: Atmospheres*, 122, 9903–9926, 2017a.
- Barrett, A. I., Hogan, R. J., and Forbes, R. M.: Why are mixed-phase altocumulus clouds poorly predicted by large-scale models? Part 2. Vertical resolution sensitivity and parameterization, *Journal of Geophysical Research: Atmospheres*, 122, 9927–9944, 2017b.
- Christensen, M. W., Carrió, G. G., Stephens, G. L., and Cotton, W. R.: Radiative impacts of free-tropospheric clouds on the properties of
10 marine stratocumulus, *Journal of the Atmospheric Sciences*, 70, 3102–3118, 2013.
- Curry, J. and Herman, G.: Relationships between large-scale heat and moisture budgets and the occurrence of Arctic stratus clouds, *Monthly Weather Review*, 113, 1441–1457, 1985.
- Fleishauer, R. P., Larson, V. E., and Vonder Haar, T. H.: Observed microphysical structure of midlevel, mixed-phase clouds, *Journal of the Atmospheric Sciences*, 59, 1779–1804, 2002.
- 15 Fridlind, A. M., Van Diedenhoven, B., Ackerman, A. S., Avramov, A., Mrowiec, A., Morrison, H., Zuidema, P., and Shupe, M. D.: A FIRE-ACE/SHEBA case study of mixed-phase Arctic boundary layer clouds: Entrainment rate limitations on rapid primary ice nucleation processes, *Journal of the Atmospheric Sciences*, 69, 365–389, 2012.
- Hall, W. and Pruppacher, H.: The survival of ice particles falling from cirrus clouds in subsaturated air, *Journal of the Atmospheric Sciences*, 33, 1995–2006, 1976.
- 20 Hobbs, P. V. and Rangno, A. L.: Microstructures of low and middle-level clouds over the Beaufort Sea, *Quarterly Journal of the Royal Meteorological Society*, 124, 2035–2071, 1998.
- Houze Jr, R. A.: *Cloud dynamics*, vol. 53, Academic press, 1993.
- Hyland, R. and Wexler, A.: Formulations for the thermodynamic properties of dry air from 173.15 to 473.15 K, at pressure to 5 MPa, 1983.
- Intrieri, J., Shupe, M., Uttal, T., and McCarty, B.: An annual cycle of Arctic cloud characteristics observed by radar and lidar at SHEBA,
25 *Journal of Geophysical Research: Oceans*, 107, 2002.
- Khvorostyanov, V., Curry, J., Pinto, J., Shupe, M., Baker, B., and Sassen, K.: Modeling with explicit spectral water and ice microphysics of a two-layer cloud system of altostratus and cirrus observed during the FIRE Arctic Clouds Experiment, *Journal of Geophysical Research: Atmospheres*, 106, 15 099–15 112, 2001.
- Klein, S. A., McCoy, R. B., Morrison, H., Ackerman, A. S., Avramov, A., Boer, G. d., Chen, M., Cole, J. N., Del Genio, A. D., Falk, M.,
30 et al.: Intercomparison of model simulations of mixed-phase clouds observed during the ARM Mixed-Phase Arctic Cloud Experiment. I: Single-layer cloud, *Quarterly Journal of the Royal Meteorological Society*, 135, 979–1002, 2009.
- Korolev, A.: Limitations of the Wegener–Bergeron–Findeisen mechanism in the evolution of mixed-phase clouds, *Journal of the Atmospheric Sciences*, 64, 3372–3375, 2007.
- Krämer, M., Schiller, C., Afchine, A., Bauer, R., Gensch, I., Mangold, A., Schlicht, S., Spelten, N., Sitnikov, N., Borrmann, S., et al.: Ice supersaturations and cirrus cloud crystal numbers, *Atmospheric Chemistry and Physics*, 9, 3505–3522, 2009.
- Küchler, N., Kneifel, S., Löhnert, U., Kollias, P., Czekala, H., and Rose, T.: A W-Band Radar–Radiometer System for Accurate and Continuous Monitoring of Clouds and Precipitation, *Journal of Atmospheric and Oceanic Technology*, 34, 2375–2392, 2017.

- Lamb, D. and Verlinde, J.: Physics and chemistry of clouds, Cambridge University Press, 2011.
- Liu, Y., Key, J. R., Ackerman, S. A., Mace, G. G., and Zhang, Q.: Arctic cloud macrophysical characteristics from CloudSat and CALIPSO, *Remote Sensing of Environment*, 124, 159–173, 2012.
- Loewe, K., Ekman, A. M., Paukert, M., Sedlar, J., Tjernström, M., and Hoose, C.: Modelling micro-and macrophysical contributors to the
5 dissipation of an Arctic mixed-phase cloud during the Arctic Summer Cloud Ocean Study (ASCOS), *Atmospheric Chemistry and Physics*, 17, 6693–6704, 2017.
- Luo, Y., Xu, K.-M., Morrison, H., McFarquhar, G. M., Wang, Z., and Zhang, G.: Multi-layer Arctic mixed-phase clouds simulated by a cloud-resolving model: Comparison with ARM observations and sensitivity experiments, *Journal of Geophysical Research: Atmospheres*, 113, 2008.
- 10 Maturilli, M.: High resolution radiosonde measurements from station Ny-Ålesund (2017-04,05,06), <https://doi.org/10.1594/PANGAEA.879767>, <https://doi.org/10.1594/PANGAEA.879820>, <https://doi.org/10.1594/PANGAEA.879822>, 2017.
- Mioche, G., Jourdan, O., Delanoë, J., Gourbeyre, C., Febvre, G., Dupuy, R., Monier, M., Szczap, F., Schwarzenboeck, A., and Gayet, J.-F.:
15 Vertical distribution of microphysical properties of Arctic springtime low-level mixed-phase clouds over the Greenland and Norwegian seas, *Atmospheric Chemistry and Physics*, 17, 12 845–12 869, 2016.
- Mitchell, D. L.: A model predicting the evolution of ice particle size spectra and radiative properties of cirrus clouds. Part I: Microphysics, *Journal of the atmospheric sciences*, 51, 797–816, 1994.
- Mitchell, D. L.: Use of mass-and area-dimensional power laws for determining precipitation particle terminal velocities, *Journal of the atmospheric sciences*, 53, 1710–1723, 1996.
- 20 Morrison, H., De Boer, G., Feingold, G., Harrington, J., Shupe, M. D., and Sulia, K.: Resilience of persistent Arctic mixed-phase clouds, *Nature Geoscience*, 5, 11–17, 2012.
- Nygård, T., Valkonen, T., and Vihma, T.: Characteristics of Arctic low-tropospheric humidity inversions based on radio soundings, *Atmospheric Chemistry and Physics*, 14, 1959–1971, 2014.
- Ovchinnikov, M., Ackerman, A. S., Avramov, A., Cheng, A., Fan, J., Fridlind, A. M., Ghan, S., Harrington, J., Hoose, C., Korolev, A.,
25 et al.: Intercomparison of large-eddy simulations of Arctic mixed-phase clouds: Importance of ice size distribution assumptions, *Journal of Advances in Modeling Earth Systems*, 6, 223–248, 2014.
- Paukert, M. and Hoose, C.: Modeling immersion freezing with aerosol-dependent prognostic ice nuclei in Arctic mixed-phase clouds, *Journal of Geophysical Research: Atmospheres*, 119, 9073–9092, 2014.
- RS41: Vaisala Radiosonde RS41-SGP, <https://www.vaisala.com/sites/default/files/documents/WEA-MET-RS41-Datasheet-B211321EN.pdf>, last visited 2018-07-24, 2017.
30
- RS92: Vaisala Radiosonde RS92-SGP, <https://www.vaisala.com/sites/default/files/documents/RS92SGP-Datasheet-B210358EN-F-LOW.pdf>, last visited 2018-07-24, 2013.
- Shupe, M. D.: Clouds at Arctic atmospheric observatories. Part II: Thermodynamic phase characteristics, *Journal of Applied Meteorology and Climatology*, 50, 645–661, 2011.
- 35 Shupe, M. D. and Intrieri, J. M.: Cloud radiative forcing of the Arctic surface: The influence of cloud properties, surface albedo, and solar zenith angle, *Journal of Climate*, 17, 616–628, 2004.
- Sommer, M., Dirksen, R., and Immler, F.: RS92 GRUAN Data Product Version 2 (RS92-GDP.2), GRUAN Lead Centre, <https://doi.org/10.5676/GRUAN/RS92-GDP.2>, 2012.

- Spichtinger, P., Gierens, K., and Read, W.: The statistical distribution law of relative humidity in the global tropopause region, *Meteorologische Zeitschrift*, 11, 83–88, 2002.
- Spichtinger, P., Gierens, K., and Read, W.: The global distribution of ice-supersaturated regions as seen by the Microwave Limb Sounder, *Quarterly Journal of the Royal Meteorological Society*, 129, 3391–3410, 2003.
- 5 Treffisen, R., Krejci, R., Ström, J., Engvall, A.-C., Herber, A., and Thomason, L.: Humidity observations in the Arctic troposphere over Ny-Ålesund, Svalbard based on 15 years of radiosonde data, *Atmospheric Chemistry and Physics*, 7, 2721–2732, 2007.
- Tsay, S.-C. and Jayaweera, K.: Physical characteristics of Arctic stratus clouds, *Journal of Climate and Applied Meteorology*, 23, 584–596, 1984.
- Verlinde, J., Harrington, J. Y., Yannuzzi, V., Avramov, A., Greenberg, S., Richardson, S., Bahrmann, C., McFarquhar, G., Zhang, G., Johnson, N., et al.: The mixed-phase Arctic cloud experiment, *Bulletin of the American Meteorological Society*, 88, 205–221, 2007.
- 10 Verlinde, J., Rambukkange, M. P., Clothiaux, E. E., McFarquhar, G. M., and Eloranta, E. W.: Arctic multilayered, mixed-phase cloud processes revealed in millimeter-wave cloud radar Doppler spectra, *Journal of Geophysical Research: Atmospheres*, 118, 2013.
- Wendisch, M., Brückner, M., Burrows, J., Crewell, S., Dethloff, K., Ebell, K., Lüpkes, C., Macke, A., Notholt, J., Quaas, J., et al.: Understanding causes and effects of rapid warming in the Arctic, *Eos*, 98, <https://doi.org/10.1029/2017EO064803>, 2017.
- 15 Westbrook, C. D., Hogan, R. J., and Illingworth, A. J.: The capacitance of pristine ice crystals and aggregate snowflakes, *Journal of the Atmospheric Sciences*, 65, 206–219, 2008.
- Whale, T. F.: Ice Nucleation in Mixed-Phase Clouds, in: *Mixed-Phase Clouds*, pp. 13–41, Elsevier, 2018.